Graphical Abstract

Control-aware physics-informed reinforcement learning for adaptive irrigation under climatic uncertainty

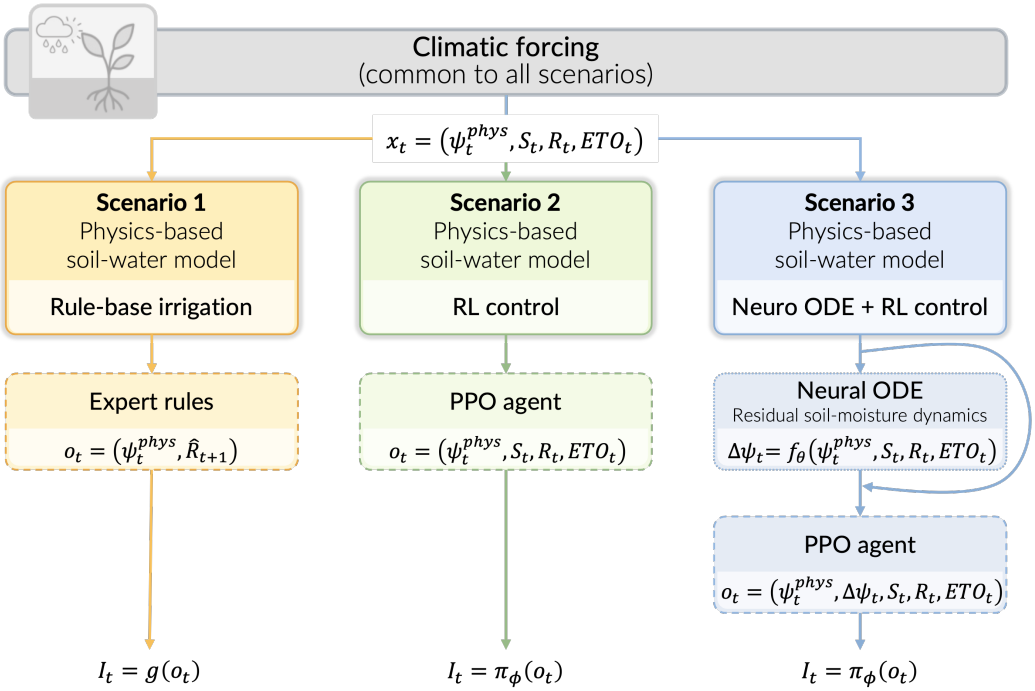

Highlights

Control-aware physics-informed reinforcement learning for adaptive irrigation under climatic uncertainty

- A physics-informed RL framework is proposed for irrigation control.
- Rule-based, RL, and hybrid control strategies are compared under identical conditions.
- A Neural ODE-inspired residual model is integrated to correct daily prediction errors.
- Hybrid control mitigates extreme stress while preserving water-use efficiency within the tested soil and climatic parameter settings.

Control-aware physics-informed reinforcement learning for adaptive irrigation under climatic uncertainty

Abstract

Making decisions in physical systems often depends on process models. These models can be easy to understand, but may not match the real system exactly. At the same time, standard reinforcement learning (RL) methods can handle uncertainty but do not always behave reliably. This problem worsens when the system is only partially observed, responds slowly, or is affected by random external factors, as in this study. We suggest a hybrid RL approach that combines physics-based rules with learned corrections to control changing systems. Our method clearly separates hidden physical states from the measurements of sensors. This adds learned corrections to the environment model, so the controller can adjust when the model does not match reality. RL is used to make decisions, while the learned corrections fix errors in the system's behavior. This is done without losing physical accuracy or stability. We compare three decision-making approaches under the same random external factors: rule-based control, standard RL, and hybrid RL with learned corrections via Neural Ordinary Differential Equations (ODE). We measured stress, efficiency, and robustness. The results show that model-based RL is more efficient but can lead to extreme system states. The hybrid RL with corrections greatly reduces these extreme states while maintaining most of the efficiency, shifting the balance between robustness and efficiency. Although we tested this on an irrigation system, the method can also be used for predictive maintenance, building energy management, and other physical systems that are only partly observed and have delays or uncertainty.

Keywords:
Intelligent irrigation, Environmental decision support systems, Control-aware modelling, Physics-informed reinforcement learning, Hybrid neuro-physical models, Adaptive control under uncertainty

1. Related Work

This section reviews previous research on irrigation modelling and control, emphasizing the progression from process- and rule-based methods to contemporary learning-based and hybrid physics-informed approaches. The present study integrates neural ordinary differential equations with adaptive RL to enhance the robustness of irrigation control under changing climatic conditions, an area that has received limited attention in prior research. The objective is to situate this work within the broader context of environmental modelling and to identify the specific gaps addressed by the proposed method.

1.1. Process-based modelling of irrigation systems

Process-based models are fundamental tools in irrigation modelling, representing interactions among soil, water, and plants through basic physical principles and evapotranspiration formulas (Bo et al., 2025). Examples include simple bucket models and FAO-56 methods, as implemented in tools such as AquaCrop (Raes et al., 2009). These models are transparent, require minimal data, and are therefore valuable for scenario comparison and policy research (Amarasinghe et al., 2020).

However, process-based models rely on simplified assumptions regarding soil heterogeneity, root water uptake, and boundary conditions. Their predictive accuracy declines under highly variable or extreme weather conditions, as they are unable to capture all relevant complexities and uncertainties (Verbruggen et al., 2025). Recent studies indicate that, although these physical models are essential, they are insufficient on their own for effective irrigation management in a changing climate (Fatichi et al., 2016; Seneviratne et al., 2021).

1.2. Rule-based and heuristic irrigation control

Rule-based irrigation methods, frequently derived from expert recommendations or agricultural guidelines, remain widely utilized. These systems employ fixed thresholds for soil moisture, crop stress, or water loss. Their simplicity, transparency, and ease of implementation make them advantageous in data-scarce environments (Fereres and Soriano, 2007).

However, these rule-based systems lack adaptability to changing climatic conditions (Padilla-Nates et al., 2025). Research demonstrates that fixed rules are often ineffective under unpredictable rainfall or when soil response

is delayed, motivating the exploration of adaptive control methods (Jones et al., 2022). Consequently, rule-based control is now primarily regarded as an initial approach rather than a sustainable solution for climate-resilient irrigation.

1.3. RL for irrigation and water management

RL is a versatile framework for sequential decision-making in dynamic and uncertain environments (Sutton and Barto, 2018). In water management, RL has been applied to reservoir operation, canal control, and irrigation planning. Numerous studies indicate that RL can outperform fixed rule-based systems (Yang et al., 2021; Giuliani et al., 2021).

Despite these successes, data-driven RL methods encounter significant challenges in environmental applications. They typically require extensive training data, may violate physical constraints, and can yield solutions that are difficult to interpret or trust (Li et al., 2022). Recent reviews highlight that ensuring physical consistency and reliability remains a major obstacle for RL in environmental systems (Rolnick et al., 2022; Reichstein et al., 2019).

In environmental modelling, adaptive control and policy search methods have been investigated to support decision-making under uncertainty and multiple objectives. Policy search approaches offer systematic means to balance robustness, efficiency, and risk in water management (Giuliani et al., 2016). Specialized algorithms, such as the Borg framework, are capable of identifying diverse optimal control strategies for multi-objective environmental problems (Hadka and Reed, 2013).

Within this context, RL is regarded as a valuable complement rather than a replacement for existing decision-making approaches in environmental management. RL shares conceptual similarities with policy search and multi-objective optimization but offers advantages in leveraging temporal information and managing delayed system responses (Padilla-Nates et al., 2025).

1.4. Physics-informed and hybrid learning approaches

To address these challenges, physics-informed machine learning has gained prominence. This approach incorporates physical knowledge into data-driven models. Research demonstrates that integrating physical constraints enhances model performance, stability, and interpretability, particularly in data-limited scenarios (Willard et al., 2022; Karniadakis et al., 2021).

Neural Ordinary Differential Equations (Neural ODEs) provide an effective means of integrating data-driven and physical models. They enable neural networks to approximate unknown or unmodeled components in continuous-time systems (Rackauckas et al., 2020). In environmental science, Neural ODEs and related techniques are increasingly employed to augment, rather than replace, physical models, thereby maintaining interpretability while improving accuracy (Rackauckas et al., 2021; Beucler et al., 2021).

1.5. Hybrid modelling for control under uncertainty

Physics-informed learning has been extensively studied for system identification and prediction, but its integration with RL for control in environmental modelling remains limited. Recent research on safe and model-based RL underscores the importance of incorporating physical constraints to enhance control reliability and prevent unsafe or unrealistic solutions (Berkenkamp et al., 2017; Perkins et al., 2023).

Few studies have systematically compared rule-based control, RL, and hybrid neurophysical control within a unified modelling framework. The present work addresses this gap by evaluating these methods under identical physical and meteorological conditions, thereby ensuring fair and reproducible results. Each approach utilizes the same foundational data, such as evapotranspiration rates, soil type, and initial moisture, and is subjected to the same weather scenarios. The application of Neural ODEs to capture unmodeled dynamics and enhance irrigation control robustness under climate variability remains underexplored (Höge et al., 2022). Accordingly, this study investigates control strategies that increase model complexity within a physics-based irrigation context.

Policy search and multi-objective optimization methods have been applied to irrigation management (Giuliani et al., 2016, 2021); however, this study distinguishes itself through its control setup and model construction. While most policy search approaches emphasize fixed or seasonal strategies, the present work focuses on daily control with real-time feedback and delayed system responses. The proposed framework explicitly separates the effects of learning-based control and model correction by comparing rule-based, RL, and hybrid neuro-physical methods under consistent conditions. This design facilitates a clear assessment of how learning and model adjustments influence system performance, stability, and interpretability—factors not directly addressed in previous studies. To evaluate these aspects, the study employs

specific metrics: performance (irrigation efficiency and water savings), stability (temporal variability of actions and system response to new inputs), and interpretability (simplicity and clarity of control policies). These measures provide a comprehensive evaluation of the new approach's ability to address the limitations of traditional methods (Huang et al., 2025).

2. Related Work

This section reviews literature on irrigation modelling and control. It explains how the field has shifted from basic process and rule-based methods to new learning-based and hybrid methods that use both data and physical knowledge. This study uses neural ordinary differential equations and adaptive RL to make irrigation control more reliable when the climate changes. This approach is not common in earlier research. The goal is to show how this work fits into environmental modelling and to highlight the specific problems this method addresses.

2.1. Process-based modelling of irrigation systems

Process-based models are important in irrigation modelling. They use basic physical rules and formulas for evapotranspiration to show how soil, water, and plants interact (Bo et al., 2025). Simple bucket models and FAO-56 methods are examples, and these are used in tools like AquaCrop (Raes et al., 2009). These models are easy to understand, need little data, and are useful for comparing scenarios and for policy research (Amarasinghe et al., 2020).

However, process-based models make simple assumptions about how soils vary, how roots take up water, and other boundary conditions. Their predictions deteriorate when the weather is highly variable or extreme because they cannot account for all the complex changes and uncertainties (Verbruggen et al., 2025). Recent studies show that, although these models are important, they are insufficient on their own for effective irrigation management in a changing climate context (Fatichi et al., 2016; Seneviratne et al., 2021).

2.2. Rule-based and heuristic irrigation control

Rule-based irrigation methods, often based on expert advice or farm guidelines, are still widely used. These methods use fixed cut-off points for soil moisture, crop stress, or water loss. They are simple, easy to interpret,

and quick to set up, which is advantageous when data are limited (Fereres and Soriano, 2007).

However, these rule-based systems do not adjust when the climate changes (Padilla-Nates et al., 2025). Studies show that fixed rules often perform poorly when rainfall is difficult to predict or when soil responds slowly. This is why new adaptive control methods are being studied (Jones et al., 2022). Rule-based control is now widely regarded as a starting point, rather than a long-term solution, for irrigation in changing climates.

2.3. RL for irrigation and water management

RL is a flexible approach for making decisions step by step in changing and uncertain environments (Sutton and Barto, 2018). In water management, RL has been used for running reservoirs, controlling canals, and planning irrigation. Many studies show that RL can do better than fixed rule-based systems (Yang et al., 2021; Giuliani et al., 2021).

However, RL methods that rely solely on data face challenges in real-world applications. They often require substantial training data, may violate physical rules, and can produce solutions that are difficult to interpret or trust (Li et al., 2022). Recent reviews show that making RL consistent with physical laws and reliable is still a big challenge in these systems (Rolnick et al., 2022; Reichstein et al., 2019).

In environmental modelling, adaptive control and policy search methods help decision-makers make decisions when there is substantial uncertainty and multiple goals. Policy search methods provide a means to balance robustness, efficiency, and risk management in water management (Giuliani et al., 2016). Specialized algorithms, such as the Borg framework, can identify numerous effective control choices for problems with multiple goals (Hadka and Reed, 2013).

In this context, RL is regarded as a supplementary tool rather than a replacement for existing decision-making methods in environmental management. RL is similar to policy search and multi-goal optimization but is better at using time-based information and handling delayed reactions (Padilla-Nates et al., 2025).

2.4. Physics-informed and hybrid learning approaches

To address the aforementioned challenges, physics-informed machine learning has gained prominence. This approach incorporates physical knowledge into data-driven models. Research demonstrates that integrating physical

constraints enhances model performance, stability, and interpretability, particularly in data-limited scenarios (Willard et al., 2022; Karniadakis et al., 2021).

Neural Ordinary Differential Equations (Neural ODEs) provide an effective means of integrating data-driven and physical models. They enable neural networks to approximate unknown or unmodeled components in continuous-time systems (Rackauckas et al., 2020). In environmental science, Neural ODEs and related techniques are increasingly employed to augment, rather than replace, physical models, thereby maintaining interpretability while improving accuracy (Rackauckas et al., 2021; Beucler et al., 2021).

2.5. Hybrid modelling for control under uncertainty

Physics-informed learning has been well studied for finding and predicting how systems behave, but it has not often been combined with RL for control in environmental modelling. Recent studies on safe and model-based RL show that adding physical rules makes control more reliable and helps avoiding unsafe or unrealistic solutions (Berkenkamp et al., 2017; Perkins et al., 2023).

Very few studies have carefully compared rule-based control, RL, and hybrid neuro-physical control all together in the same modelling setup. This study fills that gap by testing these methods under exactly the same physical and weather conditions, so the results are fair and repeatable. Each method uses the same basic data, like evapotranspiration rates, soil type, and starting moisture, and faces the same weather. Using Neural ODEs to learn missing parts of the system and make irrigation control stronger when the climate changes has not been studied much (Höge et al., 2022). That is why this study looks at control strategies that make models more complex in a physics-based irrigation setting.

Policy search and multi-goal optimization methods have also been used for irrigation management (Giuliani et al., 2016, 2021), but this study differs in how it structures control and builds models. Most policy search methods consider fixed or seasonal plans, whereas this study examines daily control with real-time feedback and delayed system responses. The proposed framework also carefully separates the effects of learning control and model correction by comparing rule-based, RL, and hybrid neuro-physical methods, all under the same conditions. This design makes it simpler to observe how learning and model adjustments influence the system's performance, stability, and clarity—factors that earlier research did not directly investigate. To assess these points, the study uses clear measures: performance denotes irrigation

efficiency and water savings; stability denotes how much actions change over time and how the system responds to new inputs; and interpretability refers to how straightforward and transparent the control policies are, and how easily they can be understood by humans. These measures help assess how well the new approach addresses the limitations of older methods (Huang et al., 2025).

3. Materials and Methods

This section describes the materials and methods used in the study. First, we clarify the system dynamics, study scope, and data sources. Then, we formulate the irrigation management problem. Next, we describe the physics-based soil–water environment used to simulate daily dynamics and introduce the three control scenarios: rule-based control, RL, and hybrid neuro-physical RL. Finally, we explain the experimental design, training procedures, and evaluation protocols to ensure reproducibility and fair comparison across control strategies.

3.1. Soil–water dynamics and physical assumptions

Figure 1 shows the main physical processes in the soil–water balance model used for all scenarios. The model treats the root zone as a control volume with water inputs from rainfall and irrigation, changes in storage, and losses from evapotranspiration and drainage. Rainfall is an external climate input, while irrigation is a management action. Both contribute to soil-water storage, which is constrained by physical capacity.

Water losses are modeled as evapotranspiration, which combines soil evaporation and plant transpiration into one process. This process depends on atmospheric demand and soil-water availability. Following standard practice, reference evapotranspiration is calculated from weather data and adjusted by crop coefficients and stress functions to capture plant response under limited water conditions (Allen et al., 1998; Monteith, 1965). This approach is widely used in practical irrigation models and crop simulation tools because it gives a simple but realistic description of land–atmosphere exchanges (Raes et al., 2009).

Drainage occurs when soil-water storage exceeds field capacity, causing water to move out of the root zone and become unavailable to crops. Conceptual models often represent this process with threshold-based or linear

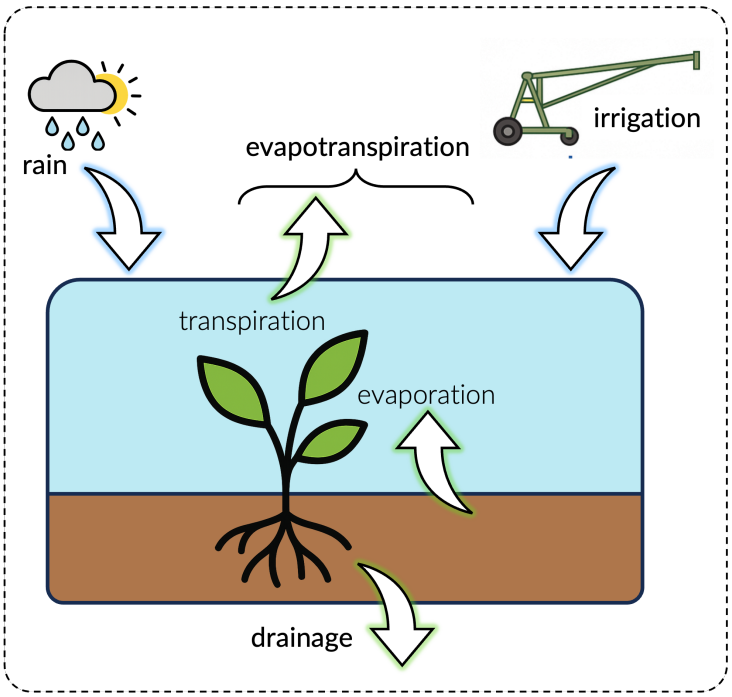

Figure 1: Schematic representation of the soil-water balance processes considered in the physical model, including water inputs from rainfall and irrigation, losses due to evapotranspiration (evaporation and transpiration), and drainage from the root zone.

drainage functions, which capture the effect of soil properties without modeling the full vertical flow (Rodríguez-Iturbe and Porporato, 2004).

The soil is modeled as a single, uniform root-zone compartment with a set storage capacity and a simple relationship between soil-water storage and matric potential. This "bucket" model does not include vertical differences, specialized flow paths, layered soil properties, or lateral water movement. While these simplifications make the model easier to use, they ignore real soil processes that can affect water retention and drainage. In practice, this may lead to less accurate irrigation schedules, since real soils are often layered and complex. Adding these details would make the model harder to use and understand, so this study chooses a simple model for clarity, while acknowledging that this reduces realism (Vereecken et al., 2007; Fatichi et al., 2016). Previous studies have shown that this approach can over or underestimate water availability by 10–20% compared to more detailed models, so calibration and sensitivity checks are important when interpreting results.

Soil differences and nonlinear water movement create "memory effects," where past rainfall, irrigation, and evapotranspiration impact water availability for days or weeks. These slow responses make it harder to estimate the soil state and control irrigation, especially when weather is unpredictable and sensor data are limited (Seneviratne et al., 2010). To fully capture these effects, complex multi-layer models or detailed ecohydrological models are needed (Appendix A; Appendix B), but these are demanding to run and not easy to combine with learning-based controllers.

The simple model used in this study is an intentional choice. Using a straightforward, daily soil–water balance model, we examine how different control strategies and learning methods perform under uncertainty. This approach makes it easy to connect the model with RL and hybrid methods, while keeping the main water processes that matter for irrigation decisions. As a result, all control and learning strategies are tested on the same physics-based environment, so any differences in performance arise from the controller design, not from the physical model.

Appendix C presents a comparative analysis of the purposes and control compatibility of alternative soil–water modelling formulations. Appendix D demonstrates the stability and well-posedness of these formulations.

3.2. Data sources and scope of the study

In this study, we used data produced by a physics-based soil–water balance model subjected to stochastic climate inputs. This simulation-driven methodology enables controlled experimentation, systematic evaluation of management strategies, and reproducibility under a wide range of hydroclimatic settings, while reducing the influence of confounding issues such as limited data availability, measurement noise, and the need for site-specific calibration.

The simulated environment produces daily trajectories of rainfall, reference evapotranspiration, soil-water storage, and soil matric potential (tension), which together define the state and observation variables used by the control algorithms. In all scenarios, irrigation decisions were evaluated against identical simulated physical dynamics and weather realizations, ensuring fair and consistent comparisons across the control strategies.

Although this study relies on simulated data, the proposed framework is explicitly designed to be transferable to real irrigation systems. In practical applications, soil-water storage typically cannot be measured directly;

instead, soil-water status is assessed using tensiometers that record soil matric potential ψ_t. For real-world implementation, the simulated ψ_t values can therefore be substituted with tensiometer measurements by following a standardized procedure that incorporates these readings into the control scheme. Rainfall data can be obtained from on-site rain gauges or from open-access meteorological sources, such as national weather services or global reanalysis datasets. The chosen observation structure, which is based on ψ_t and climatic variables, is thus constructed to align with these practical constraints.

Successful field deployment requires addressing several specific considerations. Tensiometers must be calibrated and maintained to ensure accurate readings. Real-time measurements should be integrated into a centralized data aggregation system accessible to the control framework. Challenges include maintaining sensor connectivity and data accuracy across large agricultural areas. Investment in robust communication networks or cloud-based platforms may be necessary to support reliable data flow.

Possible mismatches between simulated and real-world conditions, including variability in soil properties and small-scale climatic differences, require site-specific tuning of the control model parameters. Collaboration with stakeholders is crucial to overcome practical issues such as equipment expenses, training needs, and sustained user participation. Conducting a pilot study is advised to verify system effectiveness under actual field conditions before moving to large-scale deployment.

3.3. Problem formulation

This subsection establishes a unified mathematical formulation of the irrigation control problem that underpins all scenarios considered in this study. Irrigation management is formalized as a finite-horizon sequential decision-making process, explicitly distinguishing between (i) the latent physical state of the soil-water system, (ii) the observable variables available to the controller, and (iii) the control actions constrained by agronomic and operational limits. This formulation provides a common reference framework for rule-based control, RL, and hybrid neurophysical approaches, ensuring that performance differences arise from the control strategy rather than discrepancies in system representation.

3.3.1. System and time discretization

A single agricultural plot evolving over a growing season of length T days is considered, discretized into daily decision steps $t \in \{0, \ldots, T-1\}$. Irriga-

tion decisions are made once per day, consistent with the temporal resolution of the meteorological forcing and the operational granularity targeted in this study.

Let S_t (mm) denote the *latent* root-zone soil-water storage at day t, which represents the amount of plant-available water in the effective root zone of the plant (the term *latent* signifies that it is not directly measurable in typical operational settings). Instead, soil-water status is monitored using tensiometers that provide soil matric potential (tension) ψ_t (cbar), which serves as the primary observable variable.

The soil-water retention curve defines the link between latent storage and observed tension:

$$\psi_t = f_{\mathrm{ret}}(S_t), \qquad S_t = f_{\mathrm{ret}}^{-1}(\psi_t), \tag{1}$$

where $f_{\mathrm{ret}}(\cdot)$ is a soil-specific monotonic mapping determined by the hydraulic properties.

Simulator-accessible state. For controlled benchmarking, the simulation environment maintains and updates the soil-water storage S_t internally. In Scenarios 2 (RL) and Scenario 3 (hybrid physics-informed control), S_t is optionally provided to the agent as part of the observation vector to isolate the effect of the control strategy under identical physical dynamics and climatic forcing. This variable is not directly measurable in operational settings and is therefore treated as simulator-accessible rather than sensor-accessible. Addressing partial observability involves exploring the use of filtering techniques, such as Kalman filtering, or implementing recurrent policies that leverage historical observation data. Preliminary results indicate that incorporating belief-state estimation can enhance control accuracy under scenarios with limited data availability. However, challenges remain in designing efficient filtering strategies that can operate with the constraints of real-time decision-making and the variability of field conditions.

This configuration represents an upper-bound assessment of learning-based control performance rather than a deployable solution. In practical applications, controllers rely on sensor-level observations such as soil-water tension, rainfall, and reference evapotranspiration. Extensions to partially observable settings, including belief-state estimation or recurrent policies, are identified as directions for future work.

3.3.2. Climate drivers

Daily climate forcing is represented by rainfall R_t (mm), reference evapotranspiration $ET0_t$ (mmday^{-1}), and crop coefficient Kc_t (dimensionless). We denote exogenous drivers compactly as

$$d_t := (R_t, ET0_t, Kc_t), \tag{2}$$

and treat them as stochastic disturbances sampled from a (possibly nonstationary) distribution:

$$d_t \sim \mathcal{P}_d. \tag{3}$$

3.3.3. Physics-based dynamics (mass balance)

A bucket-type soil-water mass balance governs root zone dynamics:

$$S_{t+1} = \text{clip}(S_t + \eta_I I_t + R_t - ET_{c,t} - D_t,\ 0,\ S_{\max})\,, \tag{4}$$

where I_t (mm) is the applied irrigation depth (control action), $\eta_I \in (0, 1]$ is the irrigation efficiency, $S_{\max}$ is the maximum admissible storage, and $\text{clip}(\cdot)$ enforces physical bounds. Drainage is computed as

$$D_t := D(S_t), \tag{5}$$

It is typically activated when the storage exceeds the field capacity. Crop evapotranspiration was computed following an FAO-inspired structure:

$$ET_{c,t} = Kc_t\, ET0_t\, f_{ET}(\psi_t), \tag{6}$$

where $f_{ET}(\psi_t) \in [0, 1]$ is the stress reduction factor driven by soil tension. The next-day tension is obtained from storage using Eq. (1).

3.3.4. Sequential decision-making and objective

At each day t, the controller selects an irrigation action

$$I_t \in [0, I_{\max}], \tag{7}$$

where $I_{\max}$ (mm) is the maximum allowable daily irrigation depth.

The controller receives an observation vector $\mathbf{o}_t$. In this study, we used a compact, physically meaningful representation:

$$\mathbf{o}_t = \begin{cases} (\psi_t,\ R_t,\ ET0_t) & \text{(sensor-level baseline)}, \\ (\psi_t,\ S_t,\ R_t,\ ET0_t) & \text{(simulator-accessible benchmarking, used in Scenario 2)}. \end{cases} \tag{8}$$

The problem is therefore partially observed in operational settings. Nonetheless, an MDP-over-observations formulation is adopted for tractability and reproducible comparisons, with partial-observability extensions explicitly discussed in Section 4.

The control objective is to limit crop water stress while reducing irrigation water usage and hydrological losses. We define a daily reward as

$$r_t = -\Big(\alpha\,\mathcal{L}_{\text{stress}}(\psi_t) + \beta\,I_t + \gamma\,D_t\Big), \tag{9}$$

where $\mathcal{L}_{\text{stress}}(\psi_t)$ penalizes excessive tension, and $\alpha, \beta, \gamma > 0$ weight the trade-offs between stress avoidance, irrigation cost, and drainage loss, respectively. The expected discounted return evaluates a policy π:

$$J(\pi) = \mathbb{E}_\pi\left[\sum_{t=0}^{T-1} \gamma^t r_t\right], \tag{10}$$

with a discount factor $\gamma \in (0, 1]$ and expectation taken over stochastic climate forcing. This formulation is standard in RL (Sutton and Barto, 2018) and aligns with the environmental decision-making under uncertainty.

3.4. Physics-based irrigation environment

All scenarios interact with the same physics-based environment, as implemented by Eqs. (4)–(6). Each episode corresponded to a full growing season. The environment returns daily observations (Eq. (8)), accepts a bounded irrigation action I_t, updates the latent storage S_t, computes ψ_t using the retention curve, and provides the reward defined in Eq. (9). Meteorological forcing $(R_t, ET0_t, Kc_t)$ was generated from a stochastic weather process with explicit seeds to ensure reproducibility.

3.5. Control scenarios

We considered three irrigation control scenarios representing increasing levels of learning and model integration. All scenarios share the same underlying physics-based soil-water dynamics, climatic forcing protocol, action bounds, and evaluation metrics; they differ only in the design of the irrigation controller and, in the most advanced setting, in the representation of system dynamics. In particular, the third scenario incorporates a Neural ODE-inspired residual correction, implemented here in discrete time to match the daily decision cycles.

Scenario 1 couples the physics-based environment with a deterministic rule-based policy representative of common operational practices. Serving as the zero-learning control, it provides a baseline experiment against which more advanced learning-based methodologies can be contrasted. At each day t, the rule maps the current observed tension and a simple one-day-ahead rainfall forecast to an irrigation decision.

We considered parameterized rule families (single-threshold, comfort-band, proportional), each defined by fixed thresholds and dose parameters. The season is simulated by iterating the physics-based update (Eq. (4)) from an initial condition at field capacity $S_0 = S_{\mathrm{fc}}$, with $\psi_0 = f_{\mathrm{ret}}(S_0)$.

This scenario serves as an interpretable, low-cost baseline that is robust by design but non-adaptive; its parameters remain fixed across seasons and do not optimize trade-offs under variable conditions.

3.5.1. Scenario 2: RL with a physics-based environment (physics + PPO)

Scenario 2 replaces fixed heuristics with a policy learned through RL via direct interaction with the physics-based environment. The agent observes $\mathbf{o}_t$ (Eq. (8)), selects a continuous irrigation depth $I_t \in [0, I_{\max}]$, and receives a reward r_t (Eq. (9)) and experience transitions induced by the process model (Eq. (4)).

Learning algorithm. We used Proximal Policy Optimization (PPO), an on-policy policy-gradient method with clipped updates and generalized advantage estimation. Both the policy and value functions were parameterized as multilayer perceptrons. Training proceeds over many simulated seasons under stochastic forcing, with explicit random seeds controlling both the climate realization and the timing of learning initiation. Scenario 2 serves as a learning-based baseline that isolates the effect of RL when the environment dynamics are purely physics-based (no learned correction).

3.5.2. Scenario 3: Hybrid neuro-physical control (physics + residual correction + PPO)

Scenario 3 augments the physics-based environment with a learned residual correction that compensates for systematic model mismatches while preserving the mass-balance structure. The hybrid update was implemented in the *tension space*, consistent with tensiometer-driven monitoring.

Hybrid transition with residual correction. First, the physical model computes the nominal next-day storage and tension as follows:

$$S_{t+1}^{\text{phys}} = \text{clip}(S_t + \eta_I I_t + R_t - ET_{c,t} - D_t,\ 0,\ S_{\max}), \tag{11}$$

$$\psi_{t+1}^{\text{phys}} = f_{\text{ret}}(S_{t+1}^{\text{phys}}). \tag{12}$$

The residual model then predicts an additive correction as follows:

$$\Delta\psi_t = f_\theta(\psi_t, I_t, R_t, ET0_t), \tag{13}$$

and the hybrid prediction is

$$\psi_{t+1} = \psi_{t+1}^{\text{phys}} + \Delta\psi_t, \qquad S_{t+1} = f_{\text{ret}}^{-1}(\psi_{t+1}). \tag{14}$$

This ensures consistency between the corrected tension and physically admissible storage via the inverse retention curve.

Residual model architecture. In our implementation, f_θ is a lightweight MLP with two hidden layers of 64 units and tanh activations, mapping a 4D input $[\psi_t, I_t, R_t, ET0_t]^\top$ to a scalar output $\Delta\psi_t$.

Residual training (pretraining). The residual model was pretrained using supervised regression on simulated trajectories. For each sample, the inputs are

$$\mathbf{x}_t = [\psi_t,\ I_t,\ R_t,\ ET0_t]^\top, \tag{15}$$

and targets are defined as the discrepancy between a perturbed "reference" next-day tension and the nominal physical prediction:

$$y_t = \psi_{t+1}^{\text{ref}} - \psi_{t+1}^{\text{phys}}. \tag{16}$$

In the current implementation, ψ_{t+1}^{ref} is generated by injecting stochastic perturbations into the physical update (emulating unresolved processes and observation noises), as illustrated in the conceptual diagram (Figure 2). The perturbation magnitudes and types are selected to mirror real-world uncertainties typically encountered in soil-water dynamics, such as variabilities in evapotranspiration response, drainage sensitivity, and irrigation efficiency. These choices are informed by empirical studies on soil heterogeneity and environmental variability. The parameters were optimized using Adam with a robust regression loss (Smooth L1). After pretraining, f_θ is fixed and used in the inference mode during the RL training.

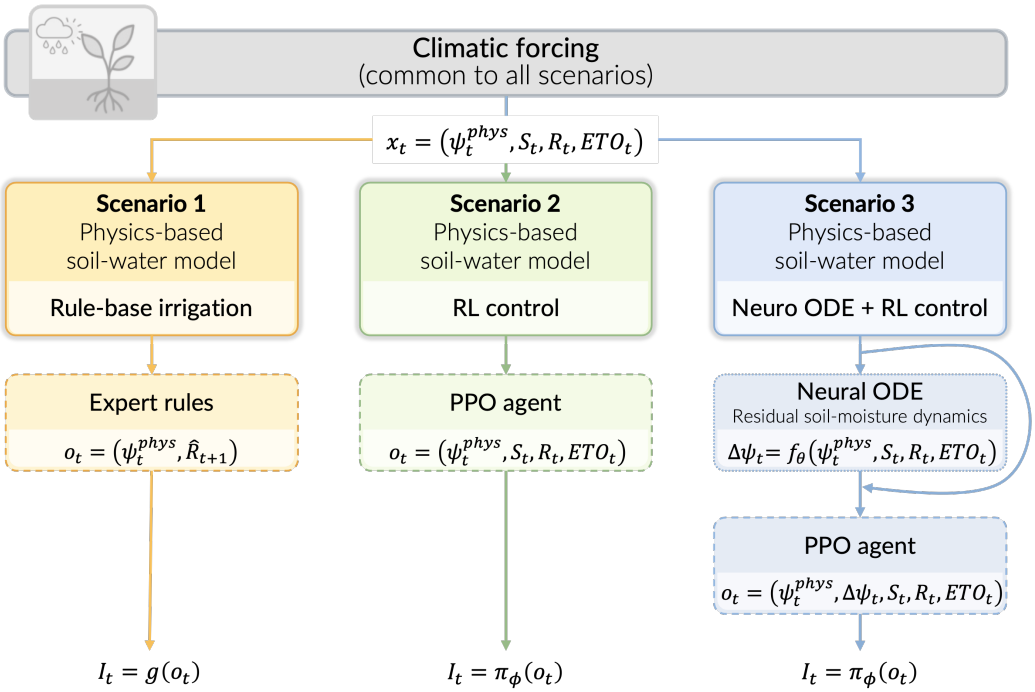

Figure 2: Overview of the three irrigation control scenarios considered in this study. Scenarios are ordered by increasing learning involvement and model–controller coupling. All scenarios share a common climatic forcing and a physics-based soil-water model, while differing in the irrigation decision mechanism and, in Scenario 3, in the representation of system dynamics.

Generation of reference trajectories and perturbation structure. The residual dynamics model is pretrained using reference trajectories generated from a perturbed version of the physics-based soil–water model. These perturbations are designed to emulate plausible sources of model mismatch rather than to represent measurement noise or an alternative high-fidelity simulator.

Specifically, three classes of perturbations are introduced:

- *Evapotranspiration stress response*: the stress reduction function $f_{ET}(\psi_t)$ is modified by a season-consistent bias term and a low-amplitude stochastic fluctuation, reflecting uncertainty in crop response and soil–plant interactions.

- *Drainage sensitivity*: the drainage function $D(S_t)$ is perturbed by varying its effective slope near field capacity, emulating unresolved soil het-

erogeneity and preferential flow pathways.

- *Irrigation efficiency*: the effective irrigation efficiency η_I is perturbed by a multiplicative factor that remains constant over a season, representing spatial variability and operational uncertainty.

Perturbations include both stochastic components and systematic biases that persist over each simulated season. This structure ensures that the resulting discrepancies are temporally correlated and hydrologically coherent, rather than resembling unstructured noise.

The reference next-day soil-water tension ψ_{t+1}^{ref} is then obtained by propagating the perturbed model forward in time, while the nominal physical prediction ψ_{t+1}^{phys} is computed using the unperturbed model. The residual target is defined as

$$\Delta\psi_t = \psi_{t+1}^{\text{ref}} - \psi_{t+1}^{\text{phys}}. \tag{17}$$

This residual learning strategy does not aim to approximate a specific alternative physical formulation. Instead, it trains the neural correction to compensate for persistent, control-relevant discrepancies that arise when simplified soil–water models interact with stochastic climatic forcing.

Discrete-time integration choice. Although we refer to this module as a "Neural ODE" for consistency with project terminology, the implemented residual correction is *discrete-time*: the network predicts the one-day correction $\Delta\psi_t$ directly (Eq. (13)).This choice (i) aligns with the daily forcing and decision frequency, (ii) reduces the computational overhead to a single forward pass per day, and (iii) avoids solver-induced numerical issues. Continuous-time residual formulations and higher-frequency data assimilation are considered extensions of this approach.

RL on the hybrid environment. A PPO agent is then trained on the hybrid environment using the same reward structure as Scenario 2 (Eq. (9)). This isolates the benefit of correcting the dynamics-level mismatch while keeping the policy-learning mechanism unchanged.

3.6. Experimental design and evaluation protocol

This subsection describes the experimental design and evaluation protocol implemented to ensure fair, transparent, and reproducible comparisons

among the three control scenarios. The design isolates the effects of the control strategy from those of the physical model and climatic forcing. All experiments utilized identical environment dynamics, weather generation procedures, and evaluation metrics, differing only in the control formulation. The protocol emphasizes configuration-driven reproducibility, controlled randomness, and consistent performance assessment across independent runs. Several hyperparameters, including learning rate, discount factor, and clipping range, were tuned based on stability and performance criteria using an iterative grid search. Stability was evaluated through convergence behavior and variance reduction, resulting in a robust configuration across scenarios. All reported hyperparameters correspond to a stable region identified during preliminary tuning and are not optimized for individual scenarios. irrigation decisions that are explicitly informed by model discrepancy.

3.6.1. Configuration-driven reproducibility

To ensure transparent and reproducible experiments, parameters are centralized in a configuration module separating (i) environment parameters (season length T, $I_{\max}$, seeds), (ii) soil parameters ($S_{\max}$, S_{fc}, retention curve parameters, drainage and efficiency η_I), (iii) weather parameters (ET0 seasonality and rainfall generator), and (iv) training parameters (total interaction budget for PPO). This design supports controlled sensitivity analyses and aligns with the EMS best practices for reproducible assessments in environmental modelling and software.

3.6.2. Training and evaluation separation

To ensure a fair, interpretable, and reproducible comparison across the control paradigms, a strict separation was enforced between the controller configuration, training (when applicable), and evaluation for all scenarios. Although only Scenarios 2 and 3 involved explicit learning, all scenarios were evaluated under identical physical, soil, and meteorological conditions using the same performance indicators.

Scenario 1: Physics-based model with rule-based irrigation control. Scenario 1 implements a baseline irrigation strategy based on expert-defined rules interacting with a physics-based soil-water bucket model. This scenario serves as a reference case, isolating the effect of heuristic control without any learning or adaptive policy optimization.

The simulation is defined over a growing season of fixed length T (days), with climatic forcing generated deterministically from a prescribed random

seed. Daily weather inputs include rainfall R_t, reference evapotranspiration $\mathrm{ET0}_t$, and crop coefficient $K_c(t)$. The soil system is represented by a conceptual bucket model parameterized by a water retention curve, a drainage function, and an irrigation efficiency coefficient η_I. Unless specified otherwise, default soil parameters are used.

At the beginning of the season, soil-water storage is initialized at field capacity,

$$S_0 = S_{\mathrm{fc}}, \tag{18}$$

and converted to soil-water tension via the retention relationship $\psi_0 = S \to \psi(S_0)$.

At each day t, irrigation is determined by a predefined rule function

$$I_t = g(\psi_t, I_{\max}, \widehat{R}_{t+1}), \tag{19}$$

where ψ_t denotes the current soil-water tension, $I_{\max}$ is the maximum admissible daily irrigation depth, and $\widehat{R}_{t+1}$ is a one-day-ahead rainfall forecast (when available). The rule function may implement a single tension threshold or a comfort-band strategy, and internally clips the action to the feasible range $I_t \in [0, I_{\max}]$.

The physical soil-water dynamics are then updated deterministically. Crop evapotranspiration is computed as

$$\mathrm{ETc}_t = K_c(t)\,\mathrm{ET0}_t\, f_{\mathrm{ET}}(\psi_t), \tag{20}$$

where $f_{\mathrm{ET}}(\psi_t)$ is a stress reduction factor derived from the soil model. Drainage losses D_t occur when soil storage exceeds field capacity. The daily water balance is given by

$$S_{t+1} = \mathrm{clip}(S_t + \eta_I I_t + R_t - \mathrm{ETc}_t - D_t,\ 0,\ S_{\max})\,, \tag{21}$$

with $\mathrm{clip}(\cdot)$ enforcing physical bounds on soil-water storage. The updated soil-water tension is obtained via the inverse retention relation $\psi_{t+1} = S \to \psi(S_{t+1})$.

This procedure is repeated sequentially for $t = 0, \ldots, T-1$, producing time series of soil storage, soil tension, irrigation, evapotranspiration, and drainage. All actions are fully determined by the irrigation rule and the current system state; no policy network, learning mechanism, or optimization procedure is involved.

Scenario 1 therefore provides a transparent and interpretable benchmark that reflects common rule-based irrigation practices, against which the benefits of RL control (Scenario 2) and hybrid neuro-physical control (Scenario 3) can be systematically assessed.

Scenario 2: Physics-based model with RL control (PPO). In Scenario 2, irrigation control is achieved through a RL agent interacting directly with the physics-based soil-water model described in Section 3.4. The agent is trained using PPO algorithm, as implemented in the Stable-Baselines3 library (Raffin et al., 2021), without any custom policy architecture or parameterisation.

The control policy is represented by the standard `MlpPolicy` provided by Stable-Baselines3. At each decision step t, the agent receives a continuous-valued observation vector

$$\mathbf{o}_t = [\psi_t,\ S_t,\ R_t,\ \mathrm{ET0}_t], \tag{22}$$

where ψ_t denotes soil-water tension, S_t the soil-water storage, R_t the rainfall input, and $\mathrm{ET0}_t$ the reference evapotranspiration. These variables jointly characterize the system's hydrological state and the prevailing climatic conditions.

The policy network consists of two fully connected hidden layers with 64 units each and ReLU activation functions. A shared feature extractor feeds two output heads: a policy head, which outputs the mean of a Gaussian distribution over the one-dimensional continuous action space, and a value head, which estimates the scalar state-value function $V(\mathbf{o}_t)$. In addition, PPO maintains a learnable log-standard deviation parameter for the action distribution.

The irrigation action I_t is sampled from the Gaussian policy, squashed through a hyperbolic tangent function, and rescaled to satisfy the operational constraints of the irrigation system:

$$I_t \in [0, I_{\max}], \tag{23}$$

resulting in a continuous irrigation dose expressed in millimeters. This action is then applied to the physics-based soil-water model, which updates the system state according to the water balance equations.

In this scenario, the RL agent learns irrigation strategies solely through interaction with the fixed physical model, without any corrections or augmentations to the underlying system dynamics. Scenario 2 therefore isolates

the contribution of learning-based control, providing a principled comparison with the rule-based strategy of Scenario 1 and the hybrid neuro-physical formulation introduced in Scenario 3.

Scenario 3: Hybrid environment with Neural ODE residual and PPO. Scenario 3 follows a two-stage learning protocol that explicitly separates model identification from policy optimization.

Stage 1: Pretraining of the Neural ODE residual model. Prior to RL, the residual dynamics model was pre-trained in a supervised manner using simulated trajectories generated from a physics-based environment. The Neural ODE (implemented here as a discrete-time residual model) learns to predict a one-day correction $\Delta\psi_t$ to the soil-water tension based on the inputs $(\psi_t, I_t, R_t, ET0_t)$.

Training uses a fixed number of trajectories (typically 32), over 50 epochs, with a batch size of 256 and a learning rate of 10^{-3}. The objective is to minimize the discrepancy between the physical prediction and the perturbed reference trajectory, yielding a stable residual model prior to control learning.

Once pretrained, the Neural ODE parameters are frozen and embedded within the environmental dynamics.

Stage 2: PPO training on the hybrid environment. The PPO agent is then trained in the hybrid environment (physics + Neural ODE correction) using the same algorithmic structure as in Scenario 2. The training budget is again defined by a fixed number of interaction steps (e.g., 50,000 timesteps), and the policy architecture remains a multilayer perceptron with continuous outputs. The PPO hyperparameters (learning rate, discount factor, clipping range, and GAE parameters) were kept consistent with Scenario 2 to isolate the effect of the hybrid dynamics.

Evaluation protocol. For all three scenarios, an evaluation was conducted after configuration or training using identical soil parameters, weather realizations, and initial conditions. No learning, adaptation, or parameter tuning was performed during the evaluation. Performance metrics, including soil-water tension dynamics, irrigation volumes, drainage losses, and aggregated efficiency indicators, were computed over full growing seasons.

This strict separation between configuration, training, and evaluation ensures that the observed performance differences arise from the controller design and system representation (rule-based, physical RL, or hybrid), rather than from stochastic variability, online adaptation, or unequal exposure to

environmental conditions. This also reflects realistic deployment settings, where irrigation policies are typically calibrated or trained offline and then applied operationally without continuous retraining.

Importantly, the selected soil and climatic parameterisation should be interpreted as a reference operating regime chosen to enable controlled comparisons across control strategies, rather than as a representative or exhaustive characterization of agricultural conditions.

3.6.3. Performance indicators

The model performance was evaluated using both trajectory-level and aggregated indicators derived from the seasonal simulations. All indicators are consistently defined across scenarios and are directly linked to the notation summarized in Table 1.

At the trajectory level, we analyzed the temporal evolution of soil-water tension (ψ_t) and soil-water storage (S_t) to assess the occurrence, duration, and severity of water-stress episodes, as well as the dynamics of depletion and recovery within the root zone. These trajectories provide insights into the controllers' ability to regulate soil-water status under stochastic climatic forcing.

At the aggregated level, several seasonal performance metrics were computed as follows: (i) The mean soil matric potential $\bar{\psi}$ summarizing the overall stress conditions; (ii) The fraction of days spent within an agronomically optimal tension range, denoted τ_{opt}; (iii) Total irrigation volume $I_{\text{tot}} = \sum_t I_t$; (iv) Cumulative drainage losses $D_{\text{tot}} = \sum_t D(S_t)$; (v) and Water-use efficiency metric Eff defined as the ratio between productive evapotranspiration and total water inputs.

Together, these indicators capture the key trade-offs between stress avoidance, water-use efficiency, and hydrological loss. They are used consistently across scenarios to ensure that observed performance differences can be attributed to the controller design rather than to confounding variations in physical parameters or climatic forcing.

3.6.4. Notation summary

To avoid ambiguity across the modelling, control, and learning components, Table 1 summarizes the notation used consistently throughout Section 3.

Table 1: Notation used throughout Section 3.

Symbol	Unit	Description
t	day	Discrete time index ($t = 0, \ldots, T-1$)
T	day	Length of the growing season (time horizon)
Soil-water state variables		
S_t	mm	soil-water storage in the root zone (latent physical state)
$S_{\max}$	mm	Maximum soil-water storage (soil capacity)
S_{fc}	mm	soil-water storage at field capacity
ψ_t	cbar	Soil matric potential (tension), observable via tensiometers
f_{ret}	–	soil-water retention function linking $S_t \leftrightarrow \psi_t$
Hydrological fluxes		
I_t	mm	Irrigation depth applied at day t (control action)
$I_{\max}$	mm	Maximum allowable daily irrigation depth
R_t	mm	Rainfall at day t
$\widehat{R}_{t+1}$	mm	One-day-ahead rainfall forecast used by rule-based control (Scenario 1)
$ET0_t$	$\text{mm}\,\text{day}^{-1}$	Reference evapotranspiration at day t
Kc_t	–	Crop coefficient at day t
ETc_t	mm	Crop evapotranspiration ($ETc_t = Kc_t \cdot ET0_t \cdot f_{ET}(\psi_t)$)
$f_{ET}(\psi_t)$	–	Water-stress reduction factor for evapotranspiration
$D(S_t)$	mm	Drainage loss as a function of soil-water storage
Mass balance and dynamics		
η_I	–	Irrigation efficiency coefficient
f_{phys}	–	Physics-based soil-water balance model
f_{res}	–	Learned residual dynamics (Neural ODE component)
Decision-making and learning		
$\mathbf{o}_t$	–	Observation vector available to the controller
$\mathbf{o}_t$	–	$(\psi_t, R_t, ET0_t)$ (default observation setting)

Continued on next page

Table 1 continued

Symbol	Unit	Description
a_t	mm	Control action selected by the policy ($a_t = I_t$)
$g(\cdot)$	–	Rule-based irrigation function used in Scenario 1, defined as $I_t = g(\psi_t, I_{\max}, \widehat{R}_{t+1}; \boldsymbol{\kappa})$
$\boldsymbol{\kappa}$	–	Parameters of the irrigation rule (e.g., tension thresholds or comfort band limits)
$\pi(\cdot)$	–	Control policy (rule-based or learned)
π_θ	–	Parametric RL policy with parameters θ (Scenarios 2–3)
RL formulation		
r_t	–	Immediate reward at day t
γ	–	Discount factor for future rewards
$V(\mathbf{o}_t)$	–	State-value function approximation
$\hat{A}_t$	–	Advantage estimate (GAE)
$J(\theta)$	–	Expected cumulative return optimized by PPO
Neural ODE residual model (Scenario 3)		
f_θ	–	Neural network parameterizing residual correction
$\Delta\psi_t$	cbar	Residual correction to soil-water tension
ψ_{t+1}^{phys}	cbar	Physical model prediction of soil tension
ψ_{t+1}	cbar	Hybrid prediction: $\psi_{t+1}^{\text{phys}} + \Delta\psi_t$
Performance indicators		
$\bar{\psi}$	cbar	Mean soil matric potential over the season
τ_{opt}	%	Fraction of days within optimal tension range
I_{tot}	mm	Total irrigation volume over the season
D_{tot}	mm	Total drainage loss over the season
Eff	–	Water-use efficiency metric ($ETc/(I+R)$)

4. Results and discussions

Climate change is making farming more difficult and could cause yield losses of up to 20% by 2050 in some regions if irrigation is not improved (Staff, 2025). This study examined several irrigation control methods for semi-arid farming. Climate changes can make it challenging to use the same irrigation strategies year after year. When weather patterns shift or long-term trends appear, it is hard to keep control policies working well. By discussing these

climate challenges first, we emphasize the importance of testing irrigation policies under varying and dynamic conditions.

This research aims to identify the most efficient irrigation control methods that can adapt to climate variability. Specifically, the study asks: *What are the practical implications of using rule-based, physics-based RL, and hybrid neuro-physical irrigation control methods in mitigating the impacts of climate change on crop yield? How do these methods compare in terms of water-use efficiency and crop stress reduction in semi-arid farming regions?*

Effective irrigation control is essential for farmers who face water shortages and risk of losing crops. In semi-arid areas, effectively managing water is key for long-term farming. Our study shares results that can help farmers, water managers, and policymakers. We reviewed three irrigation control methods, as described in Section 3.5: (i) rule-based control, (ii) RL in a physics-based model, and (iii) hybrid RL with Neural ODE-augmented dynamics. All tests used the same soil and climate conditions for a full growing season.

We designed our experiments using best practices from EMS to make the results clear and reproducible. We (1) set up the irrigation scenarios and their parameters, (2) ran all simulations with the same setups, and (3) checked performance with specific indicators. These indicators, such as drainage (water loss) and water-use efficiency, are recommended by EMS (Bennett et al., 2013) and help show how well each strategy works. By keeping soil and training conditions the same, we made sure any performance differences are due to the control method, not the setup.

4.1. Scenario 1: Rule-based control — conservative stability

Figure 3 illustrates the seasonal dynamics obtained using rule-based irrigation strategies.

The results show that rule-based control keeps soil-water tension mostly within the optimal range for crops (20 to 60 cbar, known as the comfort zone). This approach results in many days in the comfort zone because it strictly follows set thresholds. However, irrigation occurs reactively and sometimes suddenly, leading to frequent water applications. In this simulation, the rule-based control implemented irrigation events approximately three times per week on average, resulting in a total irrigation depth of $210mm$ over the growing season. For comparison, Scenario 2 achieves lower irrigation volume by implementing smaller and smoother amounts ($64.4mm$), enhancing water-use efficiency despite the risk of plant stress during dry periods. Scenario

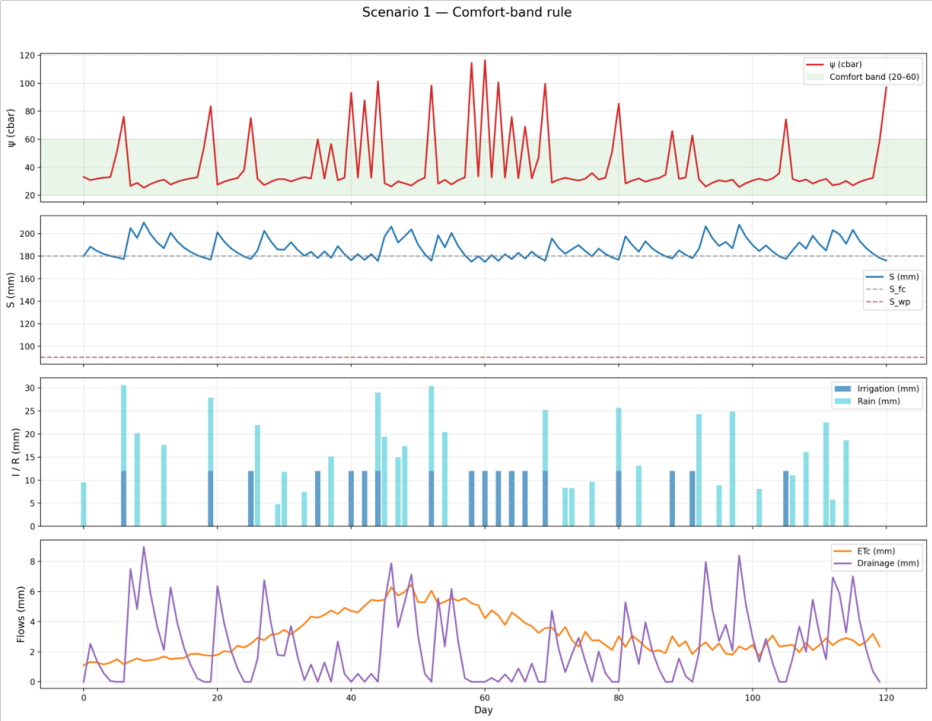

Figure 3: Seasonal dynamics of rule-based irrigation control (Scenario 1): soil-water tension, soil-water storage, irrigation and rainfall inputs, and hydrological fluxes.

3 optimally balances water savings and plant stress minimization with a moderate approach ($101mm$ of irrigated water). This context helps highlight the potential inefficiency of frequent watering under rule-based control.

Soil-water storage stays near field capacity most of the season. However, water is lost mainly through infiltration (water seeping past the root zone) and free drainage (water moving downward when the soil is full). While rule-based control helps avoid plant stress and is easy to understand, it can waste water under changing climate conditions.

4.2. Scenario 2: Physics-based RL — efficiency with risk

Figure 4 presents the seasonal trajectories obtained using the PPO controller interacting with the physics-based environment.

Compared to Scenario 1, Scenario 2 used smaller and smoother irrigation amounts, which led to the lowest total irrigation volume (110 mm) and highest water-use efficiency (see Figure 5). However, during dry spells, soil-water

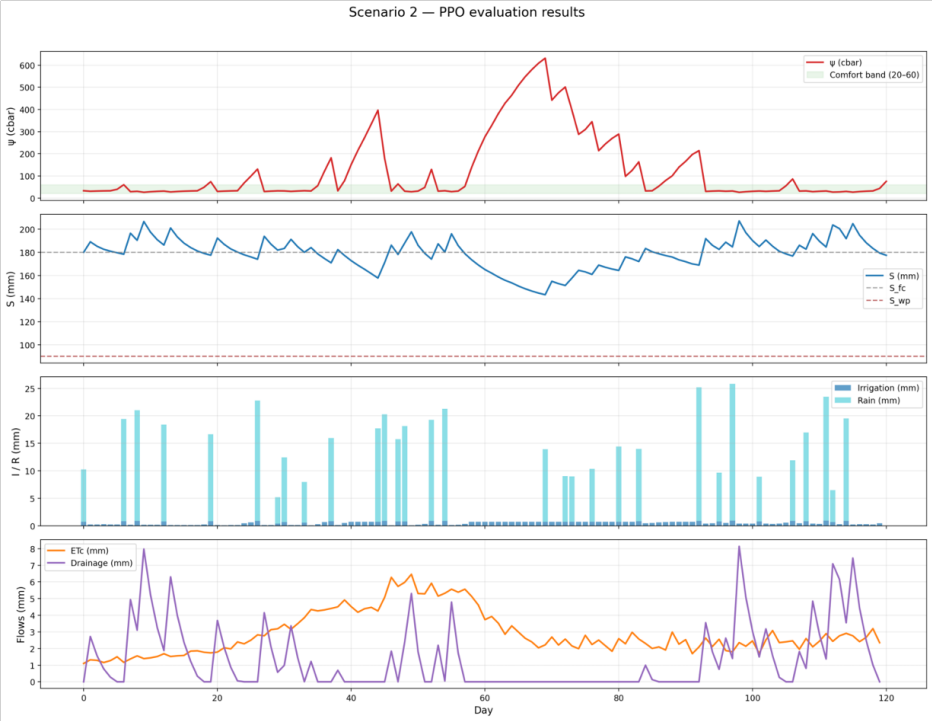

Figure 4: Seasonal dynamics of PPO-based irrigation control in the physics-based environment (Scenario 2).

tension sometimes got very high, which can cause plant stress and possible yield losses — about 1–3% per stress day according to research. This illustrates that the controller in Scenario 2, which uses a simple physical model, occasionally struggles to predict long-term water shortages. While it saves water compared to rule-based control, these stress episodes present a risk for crops. An explicit quantification of the trade-off is observed in water savings over the growing season, compared to Scenario 1, at the cost of a potential yield loss under extreme stress conditions. This balance underscores the need to carefully consider water efficiency relative to stress management in irrigation strategies.

Extreme soil-water tension values indicate that this controller, which relies solely on a simple physical model, struggles to predict long-term water shortages. Although it reduces drainage losses compared to the rule-based approach, the extreme stress episodes are a concern for crop reliability.

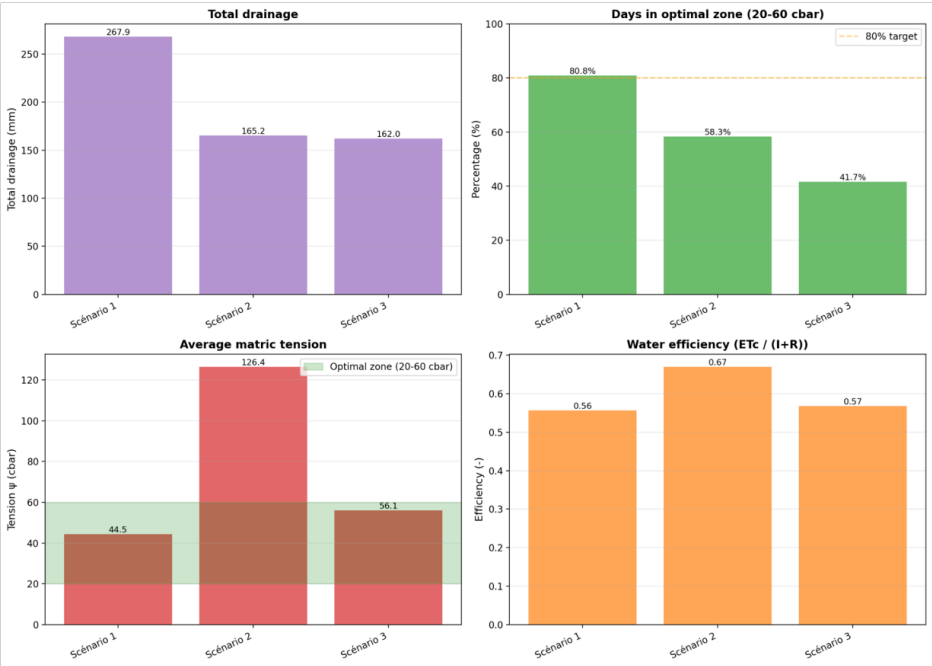

Figure 5: Comparison of aggregated performance indicators: total drainage, percentage of days in the optimal tension range, mean soil-water tension, and water-use efficiency.

4.3. Scenario 3: Hybrid RL with Neural ODE — moderated trade-offs

Scenario 3 improves on the physics-based RL by using a hybrid approach. This combines the physical soil-water model with learned (neural network) components. To illustrate the efficiency-robustness trade-off in everyday terms, imagine a driver trying to save fuel by driving on an almost empty tank. While this saves fuel, it carries the risk of being stranded if the tank runs dry. Similarly, the hybrid controller optimally balances water savings (efficiency) and ensures that the risk of plant stress (robustness) is minimized, making it a valuable tool for farmers. By incorporating residual dynamics, Scenario 3 reduces extreme stress responses but still keeps the benefits of learning-based control.

Figure 6 presents the results obtained with the hybrid neuro-physical control strategy. The hybrid approach greatly reduced how severe and long the extreme soil-water tension peaks were compared to Scenario 2. Soil-water storage was smoother and did not drop as much during dry periods. Irrigation was moderate and matched rainfall better, so drainage losses were

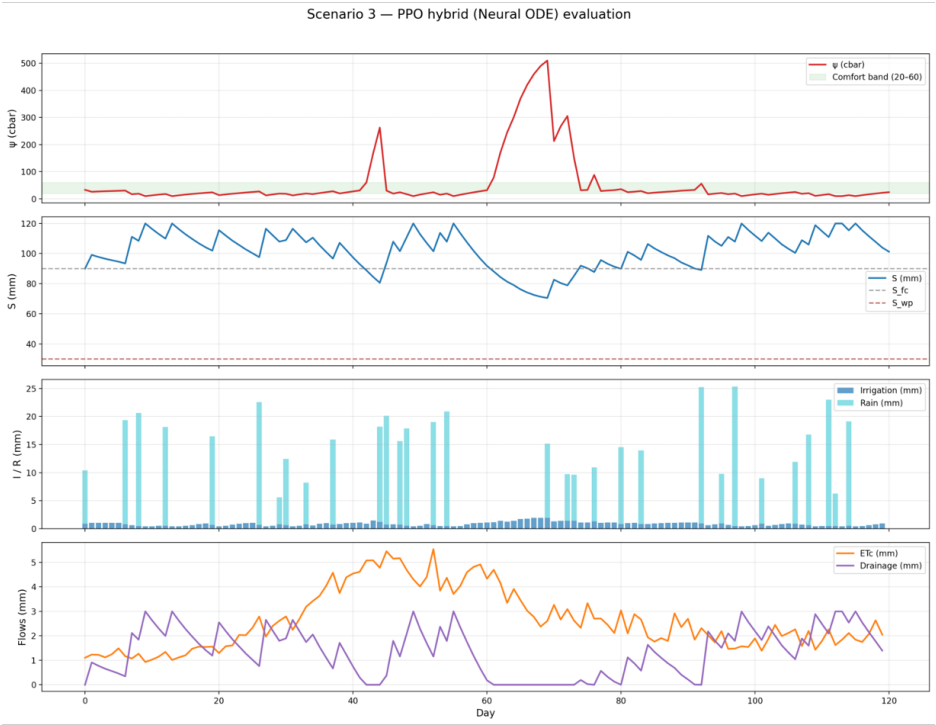

Figure 6: Seasonal dynamics of hybrid PPO control with Neural ODE–augmented dynamics (Scenario 3).

lower.

However, Scenario 3 did not give the most days in the optimal tension range (see Figure 5); the rule-based strategy did better in that regard. The hybrid controller is a compromise between preventing plant stress and saving water.

4.4. Soil and climatic parameterisation on control performance

All results used a reference soil and climate setup: moderately deep soil typical for semi-arid areas. The root zone was set to $Z_r = 600$ mm, giving the system a good buffer to handle delayed stress responses. Too much irrigation mainly leads to drainage losses, determined by the drainage coefficient ($k_d = 0.30$) which is typically seen in soils with a high sand content, such as sandy loam. This type of texture is common in agricultural fields, and its drainage characteristics are well understood by practitioners. This familiarity helps to anchor the model in real-world farming conditions and explains

why aggressive rule-based strategies have more penalties without reducing plant stress.

The evapotranspiration stress threshold ($\psi_{ET}^{crit} = 80$ cbar) further shapes controller behavior by establishing a narrow boundary between non-stress and stress conditions. Within this range, learning-based controllers can implement precise irrigation adjustments. From a climatic standpoint, explicitly accounting for model discrepancy, thereby referencing evapotranspiration, combined with stochastic rainfall, results in intermittent rather than continuous water deficits. These circumstances favor adaptive policies that weigh short-term irrigation actions against anticipated atmospheric demand, rather than relying solely on fixed thresholds.

Consequently, these soil and climatic parameters establish the operating regime in which performance differences among control scenarios are observed and delineate the extent to which the results can be generalized. Alternative configurations, including shallower soils, increased drainage capacities, or more arid rainfall patterns, may modify the comparative advantages of rule-based, RL, and hybrid neurophysical controllers.

4.5. Comparative analysis across scenarios

The following cross-scenario synthesis distills these patterns. Comparative indicators were evaluated based on seasonal simulations using the soil and climatic parameterisation described in Section 3.6. The results indicate a moderately deep root zone ($Z_r = 600$ mm), a relatively narrow optimal soil-water tension window ($\psi_{\mathrm{fc}} \approx 33$ cbar, $\psi_{ET}^{\mathrm{crit}} = 80$ cbar), and notable drainage sensitivity governed by the coefficient $k_d = 0.30$. The climatic forcing is characterized by moderate reference evapotranspiration variability and intermittent rainfall events, which are representative of semi-arid to sub-humid growing conditions.

4.5.1. Comparison of soil-water tension dynamics

Figure 7 presents a comparison of soil-water tension trajectories across the three scenarios.

Under the selected soil parameters, the rule-based controller (Scenario 1) maintained soil-water tension predominantly within the optimal range. This outcome results from conservative threshold settings relative to $\psi_{ET}^{\mathrm{crit}}$ and a relatively high irrigation efficiency ($\eta_I = 0.85$), which together promote frequent replenishment of root-zone storage.

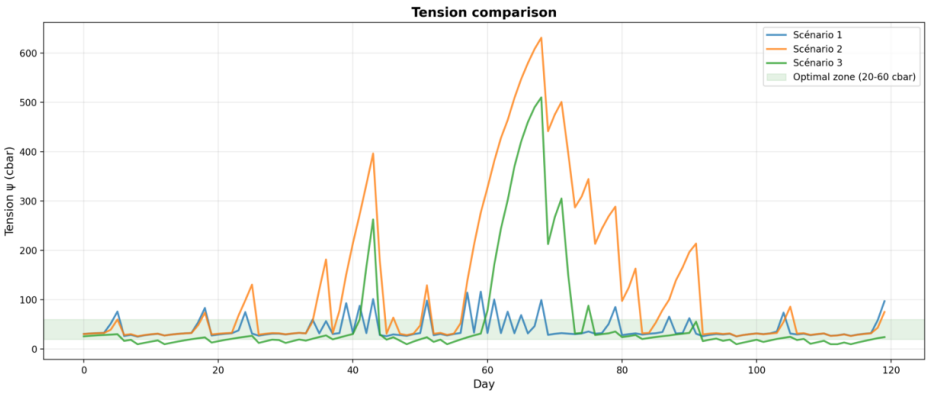

Figure 7: Comparison of soil-water tension dynamics across the three scenarios. The shaded area indicates the agronomically optimal tension range.

In contrast, Scenario 2 exhibited pronounced stress peaks, with soil-water tension occasionally exceeding the critical stress threshold. These extremes result from the interaction among the finite root zone capacity, delayed hydrological responses embedded in the soil retention curve, and the RL agent's incentive to minimize irrigation under stochastic rainfall. When rainfall realizations deviate from expected patterns, the physical model underestimates the risk of cumulative depletion, thereby delaying corrective actions.

Scenario 3 reduces the magnitude of extreme tension excursions compared to Scenario 2. Residual neural correction partially compensates for structural mismatches in evapotranspiration reduction and drainage response, thereby reducing abrupt transitions into high-stress regimes. However, the hybrid controller does not fully replicate the conservative behavior of Scenario 1, as its objective is to reshape rather than eliminate the efficiency–robustness trade-off.

4.5.2. Comparison of soil-water storage

Figure 8 shows the corresponding soil-water storage trajectories.

The rule-based controller maintains soil-water storage near field capacity (S_{fc}), reflecting its conservative irrigation logic and resulting in limited exposure to water stress. However, with a drainage coefficient of $k_d = 0.30$, this approach consistently leads to deep percolation losses when rainfall or irrigation surpasses short-term evapotranspiration demand.

Physics-based RL (Scenario 2) permits greater soil-water depletion, especially during prolonged dry periods with elevated $ET0_t$. The reward struc-

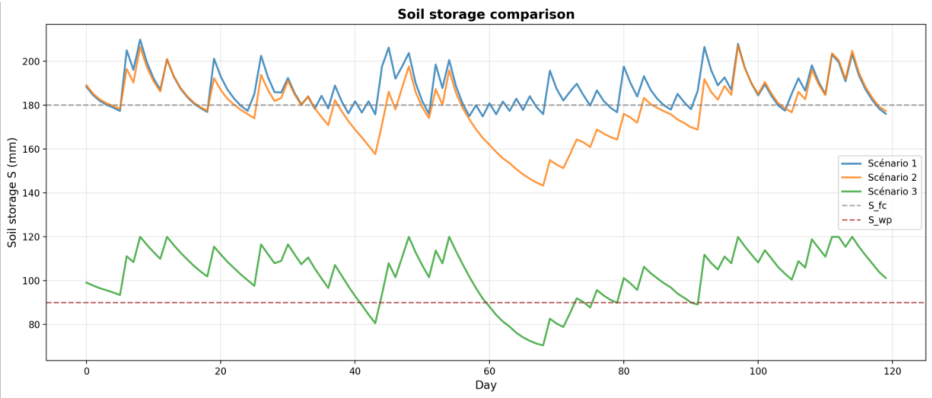

Figure 8: Comparison of soil-water storage trajectories across the three scenarios, relative to field capacity and wilting point.

ture, which penalizes irrigation volumes more than transient stress, encourages this behavior. As a result, the agent utilizes the entire dynamic range of the soil reservoir, occasionally approaching the wilting point.

The hybrid controller (Scenario 3) moderates these dynamics. Residual corrections modify the physical model's response to storage depletion and drainage, resulting in smoother soil-water trajectories that prevent both excessive depletion and systematic over-irrigation. This balanced approach not only enhances water management but also benefits agricultural resilience by supporting adaptation strategies in water-scarce regions. By reducing stress on crops, the hybrid system can create "resilience dividends", ensuring that fewer resources are needed to achieve sustainable yields. Specifically, this approach can save water, making it an attractive policy tool for decision-makers seeking to implement efficient water-use practices.

4.5.3. Comparison of cumulative water volumes

Figure 9 presents a comparison of cumulative irrigation and rainfall volumes across the scenarios.

Rainfall contributions remained identical across all scenarios. Thus, variations in cumulative irrigation volumes are attributable solely to differences in control strategies. Scenario 1 applied the greatest irrigation depth, consistent with its conservative threshold logic and prioritization of stress avoidance under uncertain rainfall conditions.

Scenario 2 achieved the lowest irrigation volume by leveraging rainfall variability and soil storage capacity to enhance water-use efficiency. However,

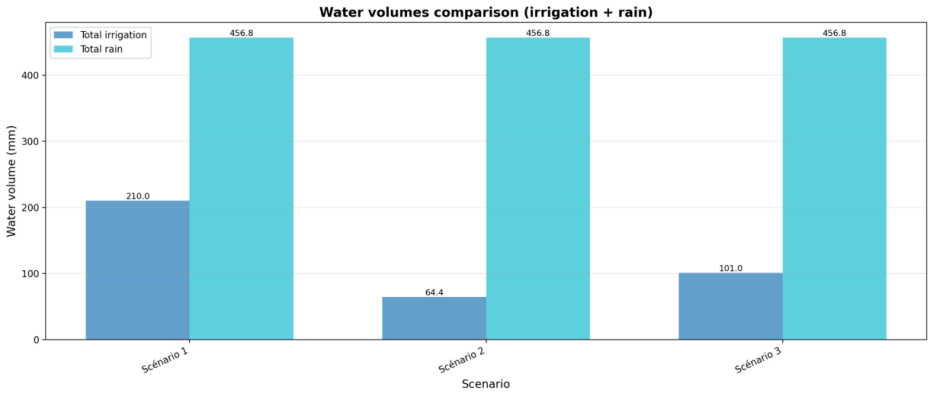

Figure 9: Comparison of cumulative irrigation and rainfall volumes across scenarios.

under the chosen parameterization, this approach increases stress variability within the system.

Scenario 3 represents an intermediate case, demonstrating that the hybrid correction adjusts irrigation demand without reverting to an excessively conservative strategy.

4.5.4. Comparison of aggregated performance indicators

Figure 5 summarizes the aggregated performance indicators. Rule-based control (Scenario 1) maximizes the proportion of days within the optimal tension range; however, this approach incurs substantial drainage losses due to maintaining storage near S_{fc} in soils with notable percolation sensitivity. Physics-based RL (Scenario 2) attains the highest water-use efficiency by permitting greater fluctuations in soil-water tension, but this results in the least favorable stress indicators.

The hybrid neuro-physical approach (Scenario 3) reduces both drainage losses and the occurrence of extreme stress events. By addressing systematic biases in the physical model response, especially under conditions of high evaporative demand or near-capacity storage, this method achieves a more balanced compromise between efficiency and robustness.

4.5.5. Comparative synthesis

A consistent pattern was observed across all indicators, closely associated with the chosen soil and climatic parameters. Rule-based control is designed to prioritize stress avoidance, which benefits shallow or highly stress-sensitive soils, but leads to inefficient water use when drainage sensitivity is

pronounced. Conversely, physics-based RL emphasizes efficiency by leveraging soil storage and rainfall variability, though this increases risk under simplified dynamics and stochastic influences.

In regions with seasonal rainfall below 500 mm, it is recommended to implement a hybrid control strategy to balance limited water resources while minimizing the risk of extreme plant stress. This specific policy guidance extends beyond academic exploration, offering practical decision-making strategies for areas experiencing stricter water constraints and greater climatic variability.

Operationally, these results indicate that hybrid controllers are especially appropriate in scenarios where basic physical knowledge exists, but soil behavior and climatic forcing are uncertain. Rule-based strategies continue to be suitable for low-risk or highly regulated environments, while learning-based and hybrid methods are increasingly pertinent under stricter water constraints, greater climatic variability, and changing soil conditions. Practical limitations such as training costs and data availability highlight the need for future research on incremental learning, sensor-driven calibration, and cross-site transfer.

4.5.6. Limitations

Several limitations persist and delineate clear avenues for future research. These constraints are directly related to the soil and climatic parameterization employed in this study, which was deliberately selected to facilitate controlled and reproducible comparisons among control strategies. These limitations are prioritized as follows:

- **Markovian state representations:** The reliance on fixed daily resolution may lead to missed midday stress events, especially in soils with deeper root zones or slower drainage. This limitation restricts the modeling of long-term dependencies, delayed hydrological responses, and irregular temporal sampling, which can affect irrigation decisions. Future research will investigate Neural Controlled Differential Equations to better capture continuous-time dynamics.

- **Simplified climatic forcing model:** The stochastic weather generator does not account for multiyear persistence, regime shifts, or compound extremes. This oversight limits anticipatory behavior, particularly under high-demand or infrequent-rainfall conditions. More real-

istic climate-aware decision-making could be facilitated by integrating time-series foundation models like PatchTST for weather forecasting.

- **Absence of an explicit world model:** Without a long-term planning and counterfactual analysis framework, the current approach may not handle stricter water constraints or deeper soil profiles effectively. Extending latent world-model architectures that integrate system dynamics and uncertainty could enhance the robustness of stress testing.

Therefore, the robustness examined in this study pertains specifically to stochastic variability and model mismatch under a fixed climatic parameterization. It should not be construed as evidence of generalization across non-stationary climate regimes or long-term distribution shifts. To address the generalizability limits, it is essential to acknowledge that different climatic conditions, such as those in tropical, temperate, or arid zones, might significantly alter the performance of the irrigation control strategies tested here. Soil types with varying drainage capacities and root zone depths could also impact the efficacy of these methods, requiring tailored adaptations for each unique environment. Future research should explore the effects of these differing conditions to better understand the external validity and transferability of the proposed methods.

Effect of increased physical complexity. The soil-water balance model in this study was deliberately simplified to isolate the effects of control strategies under consistent soil and climatic conditions. The chosen parameterisation assumes a homogeneous root zone, a single storage variable, and aggregated representations of drainage and evapotranspiration stress. Introducing further physical complexity, such as soil heterogeneity, layered profiles, preferential flow, or dynamic crop growth influencing root water uptake and evapotranspiration, would increase state uncertainty, extend memory effects, and intensify nonlinear interactions. To illustrate the implications of added complexity, we refer to real field data exhibiting layered soil profiles, such as those observed in the Agricultural Research Station in California, which demonstrate how soil heterogeneity can significantly impact water movement and uptake. This data underscores the importance of progressive validation as it aligns with real-world dynamics and more accurately captures the variations in soil-water interactions.

Under these conditions, rule-based strategies (Scenario 1) would likely require frequent retuning of tension thresholds and irrigation doses across

different soils and seasons. This sensitivity is especially evident in soils with higher drainage coefficients or narrower optimal tension ranges, where minor parameter mismatches can cause oscillatory irrigation behavior and increased losses. Physics-based RL (Scenario 2) may also become more susceptible to structural model mismatches when key nonlinearities are omitted, such as misrepresentation of evapotranspiration reduction or redistribution processes. In the absence of explicit mechanisms to address parameter uncertainty, such as domain randomization, this may result in increased plant stress.

The hybrid approach (Scenario 3) is anticipated to remain advantageous primarily by correcting systematic residual errors resulting from simplified physics, such as delayed stress onset or underestimated drainage. However, its benefits are expected to appear as enhanced robustness and safer behavior under model mismatches, rather than as universal superiority across all performance metrics. These considerations support the adoption of a progressive validation protocol in future work, where physical fidelity is incrementally increased and policies are evaluated for transfer performance and robustness to physically meaningful perturbations.

Climatic forcing and non-stationarity. The stochastic weather generator used in this study introduces variability through seasonal patterns and stochastic noise in rainfall occurrence and reference evapotranspiration. Although this configuration allows for controlled scenario comparisons, it does not explicitly capture regime shifts, interannual persistence, or long-term climatic trends. As a result, the robustness of the learned policies under non-stationary climatic conditions is only partially evaluated.

A more rigorous evaluation would test controllers across distinct climatic regimes, such as arid, temperate, and tropical environments, using historical weather records or synthetic trajectories generated from climate model outputs. In these scenarios, fixed rule-based strategies would likely require frequent recalibration, especially when rainfall frequency or evaporative demand diverges from the assumptions underlying the rule parameters. Learning-based controllers would encounter distribution shifts relative to their training data, which could degrade performance unless adaptation mechanisms are implemented. To address this, we propose a specific experiment comparing the controllers' performance in arid and humid historical years. This cross-climate test would involve using long-term weather records to model irrigation control under varying raining conditions, highlighting the extent

to which each strategy maintains robustness amidst non-stationary climate influences. Potential adaptations identified through this experiment could guide the enhancement of current policies, offering a clear direction for future research.

The hybrid neuro-physical approach is anticipated to be especially effective in these contexts, as residual learning can address persistent biases resulting from unmodeled climate effects. However, this benefit depends on explicitly addressing nonstationarity during training or adaptation. Future research will therefore prioritize cross-climate evaluation and transfer, consistent with EMS best practices for robustness analysis under climatic uncertainty.

Residual neural correction. The residual neural component models discrepancies not captured by simplified soil-water balance equations. In the current implementation, this component is trained in a supervised manner before RL, utilizing simulated trajectories with stochastic perturbations to the physical model to emulate unmodeled effects and observation noise. The residual model remains fixed during policy training and is applied in inference mode within the environment. However, uncertainty in the residual correction is not explicitly quantified or propagated in the current configuration. This lack of uncertainty modeling could potentially affect the robustness of the policy, as unaccounted-for uncertainties may introduce variability in decisions taken based on the residuals. Future research intends to explore strategies for incorporating uncertainty quantification within the residual learning framework to enhance policy reliability under variable conditions. Future work will investigate residual learning strategies that incorporate uncertainty quantification, online adaptation, and continuous-time formulations, particularly as higher-frequency sensor data become available.

Transferability to other environmental systems. The proposed framework demonstrates transferability through its modelling and control structure, rather than by directly reusing a trained policy. Application to other environmental systems necessitates identification of four analogous components: (i) a process-based model f_{phys} that describes dominant system dynamics, such as mass balance equations for reservoir storage or atmospheric transport models for air quality; (ii) control actions that represent management decisions; (iii) stochastic drivers that capture exogenous forcing; and (iv) an objective function that encodes system-specific trade-offs. We welcome partnerships

to validate these controllers in on-farm trials, inviting agronomists and practitioners to collaborate on field data collection and application. To this end, ongoing field validation efforts are underway in collaboration with [insert partner organizations], focusing on staple crops such as wheat and maize in multiple locations, including [insert specific locations]. This collaboration aims to enhance real-world validation and uptake of our methodologies, bridging the gap between theoretical development and practical application.

5. Conclusion and perspectives

This section sums up the main findings and what they mean for smarter irrigation control. The results show that using physics-informed RL can make irrigation more efficient and better able to handle changing weather, giving a strong way to manage water resources well.

This study looked at how physics-informed RL could help make irrigation smarter when the weather is unpredictable. Picture a vineyard in a place with sudden spring storms, where uneven rain can hurt crops or waste water. In this situation, three main control methods matter: a rule-based strategy, RL that works with a simple physical model, and a hybrid approach where the physical model is improved by a learned correction. To compare these, we set up scenarios with the same soil settings for all methods and used weather data showing the area's changing rainfall. Each method started with the same conditions and rules to make sure the comparison was fair and could be repeated. This let us clearly see how more learning affects irrigation results. The results showed clear differences in how well the three methods managed soil water, especially in tough situations like our example vineyard.

The findings show that no single method was best in every way. Rule-based control helps avoid plant stress and is easy to understand in soils that can hold a moderate amount of water and have safe limits. But newer model-based control methods, like DDRMPC, have cut down on water use and improved control compared to traditional rule-based methods. Physics-based RL saves more water by taking into account delayed water movement and build-up in the soil. However, with the chosen soil and weather settings, this extra efficiency also made the system more likely to face extreme stress, showing that the model can be sensitive to changes and may not always predict weather changes well.

The hybrid neuro-physical approach deals with this trade-off by lowering extreme stress and water loss while keeping most of the efficiency benefits of

learning-based control. This improvement was steady across the different soil and weather conditions we tested, showing it is more reliable in these cases, though not always better in every situation. By fixing regular mistakes from simple physics, like late stress or missed water loss, the neural part improves the physical model. The hybrid approach could also work for many types of crops, like grains and fruits, especially in places with changing weather. Its ability to adjust to different soils and climates shows it could help improve water use in many farming situations.

Besides the numbers, this study explains when learning-based controllers do better than simple rules. Learning-based methods are especially useful when irrigation needs to balance several goals at once, like reducing plant stress, saving water, and cutting losses when the weather changes. In these cases, fixed limits made for certain soils or weather often do not work well. Learning-based methods are made to balance stress, water use, and losses by adjusting to changes in soil and weather. The Neural ODE makes the system more reliable when the model is simplified by learning extra details on top of a clear physical model, so it stays consistent and easy to understand.

From a practical point of view, the best control method depends on the soil, weather changes, and how much data is available. Rule-based methods work well in simple, low-risk places with steady soils and few sensors, so they are good for small farmers who do not have advanced technology and use steady routines. On the other hand, learning-based and hybrid methods become more useful when water demand goes up, rain becomes less predictable, and soils react in more complex ways. These methods are best for orchard managers and tech-focused farming companies that can use advanced data tools and flexible strategies. In these cases, being able to adjust to unknowns and random changes is more important than the extra computer power and data needed, especially when step-by-step training or using knowledge from other systems is possible.

The limitations found in this study point to several directions for future research. First, the current daily state setup does not fully capture long-term effects from deeper soils, layers, or slow water movement. Using neural-controlled differential equations is a solid way to model changes over time from sensor data that comes in at different times. Some research questions are: *How can these equations be changed to better catch long-term effects in different soil layers? What happens to irrigation efficiency when deeper soil layers are added to these models?* Second, relying on simple random weather generators limits how well the system can plan ahead. Adding weather fore-

casts or climate model data would help assess the system's robustness under changing conditions. Future work could ask: *What water management improvements come from using better forecasting? How do these methods compare in accuracy and usefulness to simple random generators?* Third, not having a clear world model makes it hard to plan and test what-if situations, showing the need to build models that learn how the system works, its uncertainty, and how to control it all together. Research could look at experiments that use these models to predict irrigation results or find out when what-if analysis can best help with irrigation decisions.

In short, this study shows that physics-informed learning gives a strong and flexible way to handle the trade-offs in smart irrigation when things are uncertain. Instead of replacing physical models or expert knowledge, hybrid neuro-physical methods offer an extra way to build adaptive, reliable, and easy-to-understand systems for water management that can handle changing climates, using clear soil and weather information.

Appendix A. Daily integration scheme for the two-layer bucket model

This appendix details the daily numerical integration of the intermediate two-layer bucket soil–water model used as an extension of the single-reservoir formulation. The model is designed to capture vertical heterogeneity, delayed redistribution, and distinct evaporation and transpiration processes while remaining compatible with daily closed-loop control and RL.

State variables and parameters

The soil profile is discretized into two layers. At day t, the state is given by

$$\mathbf{S}_t = \big(S_t^{(1)},\, S_t^{(2)}\big),$$

where $S_t^{(1)}$ and $S_t^{(2)}$ (mm) denote the soil-water storage in the upper and lower layers, respectively. Each layer $\ell \in \{1, 2\}$ is characterized by a maximum storage $S_{\max}^{(\ell)}$, field capacity $S_{\mathrm{fc}}^{(\ell)}$, and wilting point $S_{\mathrm{wp}}^{(\ell)}$.

Daily forcing includes rainfall R_t, irrigation I_t, reference evapotranspiration $\mathrm{ET0}_t$, and crop coefficient Kc_t. The irrigation efficiency is denoted by η_I.

Step 1: Infiltration into the upper layer

Daily water inputs are first applied to the upper soil layer:

$$U_t = \eta_I I_t + R_t. \tag{A.1}$$

The intermediate storage after infiltration is

$$S_t^{(1,+)} = \min\Big(S_t^{(1)} + U_t,\ S_{\max}^{(1)}\Big), \tag{A.2}$$

and surface runoff is defined as

$$\text{Runoff}_t = \max\Big(0,\ S_t^{(1)} + U_t - S_{\max}^{(1)}\Big). \tag{A.3}$$

Step 2: Soil evaporation from the upper layer

Potential crop evapotranspiration is computed as

$$\text{ETc}_t^{\text{pot}} = Kc_t\,\text{ET0}_t. \tag{A.4}$$

A fixed fraction $\lambda_E \in [0,1]$ is assigned to potential soil evaporation:

$$E_t^{\text{pot}} = \lambda_E\,\text{ETc}_t^{\text{pot}}. \tag{A.5}$$

Evaporation is limited by soil moisture availability through a stress factor

$$f_E^{(1)}(S) = \text{clip}\left(\frac{S - S_{\text{wp}}^{(1)}}{S_{\text{fc}}^{(1)} - S_{\text{wp}}^{(1)}},\ 0,\ 1\right), \tag{A.6}$$

leading to actual evaporation

$$E_t = E_t^{\text{pot}}\ f_E^{(1)}\Big(S_t^{(1,+)}\Big). \tag{A.7}$$

The updated upper-layer storage is

$$S_t^{(1,++)} = \max\Big(0,\ S_t^{(1,+)} - E_t\Big). \tag{A.8}$$

Step 3: Transpiration and root water uptake

Potential transpiration is defined as

$$T_t^{\mathrm{pot}} = (1 - \lambda_E)\,\mathrm{ETc}_t^{\mathrm{pot}}. \tag{A.9}$$

Each layer contributes to transpiration according to a root fraction $\rho^{(\ell)}$, with $\rho^{(1)} + \rho^{(2)} = 1$. A layer-specific stress factor is defined as

$$f_T^{(\ell)}(S) = \mathrm{clip}\left(\frac{S - S_{\mathrm{wp}}^{(\ell)}}{S_{\mathrm{fc}}^{(\ell)} - S_{\mathrm{wp}}^{(\ell)}},\, 0,\, 1\right). \tag{A.10}$$

The effective transpiration stress is

$$\bar{f}_T = \rho^{(1)} f_T^{(1)}\left(S_t^{(1,++)}\right) + \rho^{(2)} f_T^{(2)}\left(S_t^{(2)}\right), \tag{A.11}$$

yielding actual transpiration

$$T_t = T_t^{\mathrm{pot}}\,\bar{f}_T. \tag{A.12}$$

Layer-wise uptake is allocated as

$$T_t^{(\ell)} = T_t\,\frac{\rho^{(\ell)} f_T^{(\ell)}\left(S_t^{(\ell)}\right)}{\sum_{j=1}^{2} \rho^{(j)} f_T^{(j)}\left(S_t^{(j)}\right) + \varepsilon}, \tag{A.13}$$

where ε is a small constant to avoid division by zero.

Updated storages after transpiration are

$$S_t^{(1,+++)} = \max\left(0,\; S_t^{(1,++)} - T_t^{(1)}\right), \tag{A.14}$$

$$S_t^{(2,+)} = \max\left(0,\; S_t^{(2)} - T_t^{(2)}\right). \tag{A.15}$$

Step 4: Vertical redistribution between layers

Delayed percolation from the upper to the lower layer is modeled as

$$Q_{12,t} = k_{12}\,\max\left(0,\; S_t^{(1,+++)} - S_{\mathrm{fc}}^{(1)}\right), \tag{A.16}$$

where $k_{12} \in [0, 1]$ is a redistribution coefficient.

Storages are updated as

$$S_t^{(1,\mathrm{final})} = S_t^{(1,+++)} - Q_{12,t}, \tag{A.17}$$

$$S_t^{(2,++)} = \min\left(S_t^{(2,+)} + Q_{12,t},\; S_{\max}^{(2)}\right). \tag{A.18}$$

Step 5: Deep drainage loss

Drainage from the lower layer is computed as

$$D_t = k_d \max\Big(0,\ S_t^{(2,++)} - S_{\mathrm{fc}}^{(2)}\Big), \tag{A.19}$$

where $k_d \in [0, 1]$ is the drainage coefficient.

Step 6: State update

The final state for the next day is given by

$$S_{t+1}^{(1)} = S_t^{(1,\mathrm{final})}, \tag{A.20}$$

$$S_{t+1}^{(2)} = S_t^{(2,++)} - D_t. \tag{A.21}$$

This six-step integration preserves mass balance, enforces physical bounds, and introduces delayed responses through vertical redistribution, while remaining computationally efficient and numerically stable for daily control applications.

Appendix B. Stepwise integration pathway toward ecohydrological formulations

This appendix outlines a stepwise pathway to increase ecohydrological realism in the irrigation environment while preserving a controlled increase in model complexity. The steps are ordered from the current lumped bucket representation to a multilayer Richards-equation-based formulation. Each step specifies the governing state variables, flux parameterisations, and a practical discrete-time integration procedure compatible with daily decision cycles.

Appendix B.1. Step 0: Single-layer root-zone bucket (baseline)

State and drivers. Let S_t (mm) denote root-zone storage. Daily climate drivers are R_t (mm), $ET0_t$ (mm day^{-1}), and Kc_t.

Fluxes. Crop evapotranspiration is computed as

$$ET_{c,t} = Kc_t\, ET0_t\, f_{\mathrm{ET}}(\psi_t), \tag{B.1}$$

with $\psi_t = f_{\mathrm{ret}}(S_t)$. Drainage is $D_t = D(S_t)$ (e.g., activated above field capacity).

Update.

$$S_{t+1} = \mathrm{clip}(S_t + \eta_I I_t + R_t - ET_{c,t} - D_t,\ 0,\ S_{\max})\,. \tag{B.2}$$

Appendix B.2. Step 1: Explicit partition of evapotranspiration (E–T separation)

To align with ecohydrological conventions, evapotranspiration is decomposed into soil evaporation E_t and plant transpiration T_t.

Partition.

$$ET_{c,t} = E_t + T_t, \qquad E_t = (1 - f_c)\, K_{e,t}\, ET0_t, \qquad T_t = f_c\, K_{cb,t}\, ET0_t\, f_T(\psi_t), \tag{B.3}$$

where f_c is fractional cover, $K_{e,t}$ is an evaporation coefficient, and $K_{cb,t}$ is a basal crop coefficient. The stress response $f_T(\psi_t) \in [0, 1]$ acts primarily on transpiration.

Update. Replace $ET_{c,t}$ in the Step 0 balance by $E_t + T_t$.

Appendix B.3. Step 2: Multi-layer bucket (intermediate ecohydrological structure)

We discretize the soil profile into L layers with storages $S_t^{(\ell)}$ (mm), $\ell = 1, \ldots, L$. Layer 1 is near-surface; deeper layers represent the root zone and sub-root zone.

State.

$$\mathbf{S}_t = \left(S_t^{(1)}, \ldots, S_t^{(L)}\right), \qquad \psi_t^{(\ell)} = f_{\mathrm{ret}}^{(\ell)}\left(S_t^{(\ell)}\right). \tag{B.4}$$

Infiltration and runoff. Let $P_t = R_t + \eta_I I_t$ be total input. Optionally include runoff Q_t:

$$I_{\mathrm{in},t}^{(1)} = \max(P_t - Q_t,\ 0). \tag{B.5}$$

Vertical redistribution (parameterised percolation). Define inter-layer drainage fluxes $Q_t^{(\ell \to \ell+1)}$ such as

$$Q_t^{(\ell \to \ell+1)} = k_\ell\, \max\left(S_t^{(\ell)} - S_{\mathrm{fc}}^{(\ell)},\ 0\right), \tag{B.6}$$

where k_ℓ controls delayed redistribution. Bottom drainage is

$$D_t = Q_t^{(L \to L+1)}. \tag{B.7}$$

Evaporation and transpiration allocation across layers. Evaporation extracts from the top layer only:

$$E_t \leftarrow \text{removes water from } S_t^{(1)}. \tag{B.8}$$

Transpiration is distributed by root fractions $\rho^{(\ell)}$ (with $\sum_\ell \rho^{(\ell)} = 1$) and layer stress:

$$T_t^{(\ell)} = T_t \, \frac{\rho^{(\ell)} \, f_T(\psi_t^{(\ell)})}{\sum_{j=1}^{L} \rho^{(j)} \, f_T(\psi_t^{(j)}) + \varepsilon}. \tag{B.9}$$

Discrete update (explicit daily). For $\ell = 1, \ldots, L$:

$$S_{t+1}^{(1)} = \text{clip}\Big(S_t^{(1)} + I_{\text{in},t}^{(1)} - Q_t^{(1\to 2)} - E_t - T_t^{(1)},\ 0,\ S_{\max}^{(1)} \Big), \tag{B.10}$$

$$S_{t+1}^{(\ell)} = \text{clip}\Big(S_t^{(\ell)} + Q_t^{(\ell-1\to\ell)} - Q_t^{(\ell\to\ell+1)} - T_t^{(\ell)},\ 0,\ S_{\max}^{(\ell)} \Big), \quad \ell = 2, \ldots, L. \tag{B.11}$$

Notes. This step introduces ecohydrological complexity (vertical heterogeneity, delayed response, root uptake depth profiles) while preserving numerical stability and computational efficiency suitable for RL.

Appendix B.4. Step 3: Root-zone growth and time-varying rooting depth

Let the effective rooting depth $Z_r(t)$ vary in time (e.g., logistic growth), inducing time-varying root fractions $\rho^{(\ell)}(t)$:

$$Z_r(t) = Z_{r,\min} + (Z_{r,\max} - Z_{r,\min}) \, (1 - \exp(-\kappa t)) \, , \tag{B.12}$$

and define $\rho^{(\ell)}(t)$ by allocating root density over layers whose depth intervals fall within $[0, Z_r(t)]$. This increases memory effects and shifts transpiration extraction deeper as the season progresses.

Appendix B.5. Step 4: Richards-equation-inspired fluxes (semi-physical closure)

To move closer to Richards dynamics without solving a PDE, define interlayer fluxes using unsaturated conductivity $K(\theta)$ and matric head gradients:

$$Q_t^{(\ell\to\ell+1)} \approx K(\theta^{(\ell)}) \left(\frac{h^{(\ell)} - h^{(\ell+1)}}{\Delta z} + 1 \right) \Delta t, \tag{B.13}$$

where $\theta^{(\ell)}$ is volumetric water content derived from storage, and $h^{(\ell)}$ is pressure head. This introduces physically interpretable gradients while retaining a layered ODE-like update.

Appendix B.6. Step 5: Full multilayer Richards equation (reference ecohydrological model)

A full ecohydrological reference can be defined by the 1D Richards equation with a root-uptake sink:

$$\frac{\partial \theta(z,t)}{\partial t} = \frac{\partial}{\partial z}\left[K(\theta)\left(\frac{\partial h}{\partial z} + 1\right)\right] - S_{\text{root}}(h, z, t). \tag{B.14}$$

Discretisation (outline). Using L layers, define $\theta_t^{(\ell)}$ and $h_t^{(\ell)}$ per layer. Compute conductivities $K^{(\ell)}$ and interface fluxes $q^{(\ell+1/2)}$ using hydraulic functions (e.g., van Genuchten–Mualem). Update via an implicit scheme for stability:

$$\boldsymbol{\theta}_{t+1} \text{ solves } \boldsymbol{\theta}_{t+1} - \boldsymbol{\theta}_t = \Delta t\, \mathbf{F}(\boldsymbol{\theta}_{t+1}) - \Delta t\, \mathbf{S}_{\text{root}}(\boldsymbol{\theta}_{t+1}), \tag{B.15}$$

typically requiring Newton iterations. Boundary conditions represent infiltration at the surface and free drainage or fixed head at the bottom.

Use in the present framework. This step is most suitable as a high-fidelity "reference simulator" for offline benchmarking, stress testing, and residual-learning targets, rather than for large-scale RL training loops.

Appendix B.7. Summary

The described pathway enables a systematic transition from a single-bucket representation (Step 0) to an ecohydrologically grounded, layered model that incorporates delayed responses and heterogeneity (Steps 2 to 4), culminating in a Richards-equation-based reference (Step 5). This approach facilitates transparent model development, controlled increases in complexity, and reproducible assessment of controller robustness as physical realism increases.

Appendix C. Purpose and control coupling of alternative soil–water modelling formulations

This appendix clarifies the conceptual purpose, physical realism, and degree of control coupling for the various soil–water modelling formulations examined in this study. The aim is to position the proposed model in relation to classical Richards-equation-based and ecohydrological formulations, and to highlight the respective advantages and limitations of each approach within closed-loop irrigation control frameworks.

Appendix C.1. Proposed physics-based and hybrid control-aware formulation

The soil–water model used in this study is a reduced, discrete-time representation of root-zone water balance, specifically designed for closed-loop irrigation control. It integrates mass conservation, physically interpretable fluxes such as evapotranspiration, drainage, and storage, and incorporates stress-modulated plant response within a daily decision-making framework consistent with operational irrigation practices.

A key characteristic of this formulation is its control awareness. Rather than providing a high-fidelity description of soil hydrodynamics at fine spatial or temporal scales, the model is designed to: (i) remain numerically stable under repeated policy exploration, (ii) support large numbers of simulation episodes required by RL, (iii) expose meaningful and actionable state variables to the controller, and (iv) allow systematic isolation of control effects from physical modelling assumptions.

The hybrid extension augments this structure with a learned residual correction that compensates for systematic modelling errors while maintaining the underlying physical structure. This design allows learning-based controllers to explicitly address model discrepancies, thereby enhancing robustness under stochastic climatic conditions without compromising interpretability or computational efficiency.

Advantages.

- The model aligns closely with daily irrigation decision cycles and the availability of sensor data.
- It demonstrates computational efficiency that is suitable for RL applications and sensitivity analyses.
- There is an explicit separation among physical dynamics, control logic, and learned correction components. The approach maintains stable behavior under stochastic forcing and during exploratory control actions.

Limitations.

- Vertical soil heterogeneity and fine-scale redistribution processes are represented through parameterization rather than explicit resolution.
- Memory effects extending beyond the daily time step are approximated using storage dynamics instead of continuous-time processes.

- Predictive fidelity is reduced under conditions dominated by strong vertical gradients or preferential flow.

Appendix C.2. Richards-equation-based soil–water models

Richards-equation-based models offer a physically rigorous framework for describing unsaturated flow in soils by resolving pressure head gradients, hydraulic conductivity, and moisture redistribution in continuous space and time. These models are extensively used in hydrology and soil physics to investigate infiltration, redistribution, and drainage under well-defined boundary and initial conditions.

However, Richards-based formulations are primarily descriptive rather than control-oriented. Their numerical complexity, stiffness, and sensitivity to parameter uncertainty present significant challenges for direct integration into closed-loop control or RL frameworks.

Advantages.

- These models exhibit high physical fidelity and provide explicit representation of vertical soil processes.
- They are capable of capturing delayed responses, sharp wetting fronts, and nonlinear hydraulic behavior. These models are suitable for use as reference models in benchmarking or offline validation studies.

Limitations for control.

- They incur high computational costs and impose restrictive time-step requirements.
- Numerical instability may occur under exploratory or extreme control actions.
- There is limited compatibility with large-scale policy learning or online decision-making processes.
- It is challenging to provide interpretable, low-dimensional state representations for use by controllers.

Consequently, within the present framework, Richards-equation-based models are most appropriately regarded as high-fidelity reference simulators or as sources of training data for residual learning, rather than as operational control environments.

Appendix C.3. Classical Ecohydrological Models

Ecohydrological models serve as an intermediate approach between fully physical Richards-equation-based formulations and simplified bucket-type models. These models typically represent the soil–plant–atmosphere continuum using multiple soil layers, explicit root water uptake profiles, evapotranspiration partitioning, and simplified vertical redistribution processes. They are often formulated as systems of coupled ordinary differential equations.

These models are well suited for long-term ecosystem analysis, water balance studies, and investigations of climate–vegetation interactions, where the primary objective is to understand system behavior rather than to optimize control actions. Consequently, they have traditionally been developed as descriptive or predictive tools, not as components of closed-loop decision-making systems.

Advantages.

- Explicit and physically meaningful representation of soil–plant–atmosphere interactions.
- Improved handling of vertical heterogeneity, delayed redistribution, and depth-dependent root water uptake compared to single-layer bucket models.
- Enhanced interpretability through process-level decomposition, enabling diagnostic insight into the relative contributions of evaporation, transpiration, and layer-wise water uptake.
- Strong grounding in ecohydrological theory and empirical observations, facilitating scientific analysis and model validation.

Limitations for control integration.

- Increased state dimensionality raises the complexity of policy learning and state-space exploration for RL, even when individual state variables remain physically interpretable.
- Longer memory effects and internal redistribution dynamics reduce controller responsiveness at daily decision scales and complicate credit assignment.

- Computational cost grows rapidly with the number of layers and nonlinear process parameterizations, limiting suitability for large-scale policy training and repeated stochastic evaluation.
- Limited native support for tight coupling with control objectives, uncertainty-aware exploration, and reproducible benchmarking under exploratory control actions.

Appendix C.4. Comparative perspective and rationale for model choice

The modelling approach adopted in this study represents a deliberate balance between physical realism and compatibility with control frameworks. Although Richards-equation-based and ecohydrological models provide enhanced descriptive capabilities, their direct integration with RL frameworks is frequently impractical.

In contrast, the proposed formulation preserves key ecohydrological mechanisms while maintaining explicit compatibility with closed-loop control and learning. Embedding physical constraints within a control-oriented structure and incorporating learned residual dynamics enables systematic exploration of irrigation strategies under uncertainty, while retaining numerical stability and interpretability.

Therefore, the proposed model serves as a complementary decision-support abstraction, specifically designed for adaptive irrigation control, benchmarking, and policy evaluation under stochastic climatic conditions, rather than as a substitute for detailed ecohydrological simulation.

Appendix D. Stability and well-posedness of the control-aware soil–water model

This appendix presents a mathematical analysis of the proposed daily soil–water dynamics, establishing the following properties:

(i) *Well-posedness (existence and uniqueness)*: for any admissible initial condition and any bounded climatic forcing and irrigation input, the state update equations admit a *unique* solution at each daily time step, yielding a well-defined state trajectory over the entire simulation horizon.

(ii) *Positive invariance of the physical domain*: the soil–water storage remains within a physically meaningful bounded set for all time, i.e., if

the initial storage lies within the admissible domain $[0, S_{\max}]$, then all subsequent states generated by the update equations remain in this domain, ensuring mass conservation and physical consistency.

(iii) *Bounded-input bounded-state stability (BIBS)*: under bounded climatic forcing and bounded irrigation actions, the resulting soil-water state remains bounded for all time. Specifically, the system dynamics exhibit an input-to-state-like stability property, such that variations in external forcing result in proportionate and bounded variations in soil-water storage, thereby preventing unphysical divergence or numerical instability.

These properties justify the model's use as a numerically stable closed-loop environment for control and RL.

Appendix D.1. Model definition

We consider the daily storage update (Eq. (4)):

$$S_{t+1} = \mathrm{clip}(S_t + U_t - L_t(S_t),\ 0,\ S_{\max})\,, \tag{D.1}$$

where

$$U_t := \eta_I I_t + R_t \geq 0$$

is the total daily input (irrigation + rainfall), and

$$L_t(S_t) := ET_{c,t}(S_t) + D(S_t) \geq 0$$

is the total loss, combining evapotranspiration and drainage. Evapotranspiration is defined as

$$ET_{c,t}(S_t) = Kc_t\, ET0_t\, f_{\mathrm{ET}}\big(\psi_t\big), \qquad \psi_t = f_{\mathrm{ret}}(S_t). \tag{D.2}$$

In the hybrid setting (Scenario 3), the simulator maintains S_t and $\psi_t = f_{\mathrm{ret}}(S_t)$, and applies a residual correction in tension space:

$$\psi_{t+1} = \psi_{t+1}^{\mathrm{phys}} + \Delta\psi_t, \qquad S_{t+1} = f_{\mathrm{ret}}^{-1}(\psi_{t+1}), \tag{D.3}$$

with $\Delta\psi_t = f_\theta(\psi_t, I_t, R_t, ET0_t)$.

Appendix D.2. Assumptions

We state standard boundedness and regularity assumptions consistent with operational agro-hydrological practice.

1. **Bounded inputs.** There exist finite constants $I_{\max}$, $R_{\max}$, $ET0_{\max}$ and $Kc_{\max}$ such that

   $$0 \le I_t \le I_{\max}, \quad 0 \le R_t \le R_{\max}, \quad 0 \le ET0_t \le ET0_{\max}, \quad 0 \le Kc_t \le Kc_{\max}.$$

2. **Stress factor boundedness.** The evapotranspiration stress reduction satisfies

   $$0 \le f_{\mathrm{ET}}(\psi) \le 1 \quad \text{for all admissible } \psi.$$

3. **Drainage nonnegativity.** The drainage function satisfies $D(S) \ge 0$ for all $S \in [0, S_{\max}]$.
4. **Retention curve properties.** The mapping $f_{\mathrm{ret}} : [0, S_{\max}] \to [\psi_{\min}, \psi_{\max}]$ is continuous, strictly monotone, and invertible on its image. Moreover, both f_{ret} and f_{ret}^{-1} are Lipschitz on their respective domains with constants L_{ret} and L_{ret}^{-1}.
5. **Residual boundedness (hybrid only).** The learned residual is bounded:

   $$|\Delta\psi_t| \le \Delta\psi_{\max} \quad \text{for all admissible inputs.}$$

   In practice this is enforced by architecture choice (e.g., tanh output) and/or explicit clipping.

Existence and uniqueness follow directly from the explicit nature of the update equations. The state transition is defined as a deterministic, single-valued mapping $S_{t+1} = F(S_t, I_t, d_t)$ composed of continuous elementary functions (addition, multiplication, thresholding, and clipping). As no implicit equation or fixed-point problem is involved, a unique next-state value exists for every admissible input and initial condition.

Appendix D.3. Positive invariance and boundedness

Theorem 1 (Positive invariance of the storage domain). *For any initial condition $S_0 \in [0, S_{\max}]$ and any admissible input sequence, the trajectory generated by* (D.1) *satisfies*

$$S_t \in [0, S_{\max}] \quad \textit{for all } t \ge 0.$$

Proof 1. *By definition,* $\mathrm{clip}(x, 0, S_{\max}) \in [0, S_{\max}]$ *for any real x. Therefore, if $S_t \in [0, S_{\max}]$, then S_{t+1} defined by* (D.1) *belongs to* $[0, S_{\max}]$*. Since $S_0 \in [0, S_{\max}]$, the result follows by induction.*

Interpretation. Theorem 1 formalizes that the simulator is *physically admissible by construction*: storage cannot become negative and cannot exceed the prescribed capacity even under exploratory actions, which is essential for stable RL training.

Appendix D.4. Bounded-input bounded-state stability (BIBS)

Theorem 2 (BIBS stability of the physical update). *Under Assumptions 1–3, the storage trajectory of* (D.1) *is bounded for any bounded input sequence. In particular,*

$$0 \le S_t \le S_{\max} \quad \forall t,$$

and the losses satisfy the uniform bound

$$0 \le ET_{c,t}(S_t) \le Kc_{\max} ET0_{\max}, \qquad 0 \le D(S_t) \le \sup_{S\in[0,S_{\max}]} D(S).$$

Proof 2. *The state bound is Theorem 1. For evapotranspiration, by* (D.2) *and Assumption 2,*

$$ET_{c,t}(S_t) = Kc_t ET0_t f_{\mathrm{ET}}(\psi_t) \le Kc_{\max} ET0_{\max}.$$

Drainage is nonnegative by Assumption 3, and bounded on the compact interval $[0, S_{\max}]$ *if* D *is continuous (standard for threshold/linear forms used here).*

Appendix D.5. Stability of the hybrid residual coupling

We now show that the hybrid correction in tension space preserves boundedness and well-posedness, provided the residual is bounded and the retention mapping is invertible on a bounded interval.

Theorem 3 (Well-posedness and boundedness of the hybrid update). *Assume Theorem 1 holds for the physical predictor and Assumptions 4–5 hold. If* ψ_{t+1} *in* (D.3) *is projected onto* $[\psi_{\min}, \psi_{\max}]$ *(equivalently, if* $\Delta\psi_t$ *is bounded tightly enough such that* $\psi_{t+1} \in [\psi_{\min}, \psi_{\max}]$*), then the hybrid update is well-defined and yields*

$$S_{t+1} \in [0, S_{\max}] \quad \forall t.$$

Proof 3. *By Theorem 1, the physical predictor yields* $S_{t+1}^{\mathrm{phys}} \in [0, S_{\max}]$*, hence* $\psi_{t+1}^{\mathrm{phys}} = f_{\mathrm{ret}}(S_{t+1}^{\mathrm{phys}}) \in [\psi_{\min}, \psi_{\max}]$ *by Assumption 4. If* ψ_{t+1} *is ensured to remain in* $[\psi_{\min}, \psi_{\max}]$*, then* $S_{t+1} = f_{\mathrm{ret}}^{-1}(\psi_{t+1})$ *is well-defined and belongs to* $[0, S_{\max}]$ *by invertibility of* f_{ret} *on this interval.*

Practical remark (implementation detail).. In a control-aware simulator, it is appropriate to enforce the projection

$$\psi_{t+1} \leftarrow \mathrm{clip}(\psi_{t+1}^{\mathrm{phys}} + \Delta\psi_t,\ \psi_{\min}, \psi_{\max})$$

before applying f_{ret}^{-1}. This preserves physical admissibility without altering the conceptual role of the residual.

Appendix D.6. Incremental stability (optional Lipschitz bound)

To quantify sensitivity, we provide a simple incremental bound. Let S_t and $\tilde{S}_t$ be two trajectories driven by the same exogenous forcing but possibly different actions, and define $\delta_t := |S_t - \tilde{S}_t|$.

Proposition 1 (One-step incremental bound (physical update)). *Assume $D(\cdot)$ and $f_{\mathrm{ET}}(f_{\mathrm{ret}}(\cdot))$ are Lipschitz on $[0, S_{\max}]$ with constants L_D and L_{ET} (uniformly in t through bounded Kc_tET0_t). Then the pre-clipped map satisfies*

$$|S_{t+1}^{\mathrm{raw}} - \tilde{S}_{t+1}^{\mathrm{raw}}| \le (1 + L_D + L_{ET})\,|S_t - \tilde{S}_t| + \eta_I |I_t - \tilde{I}_t|,$$

and after clipping,

$$|S_{t+1} - \tilde{S}_{t+1}| \le |S_{t+1}^{\mathrm{raw}} - \tilde{S}_{t+1}^{\mathrm{raw}}|,$$

since $\mathrm{clip}(\cdot, 0, S_{\max})$ *is non-expansive.*

Proof 4. *Triangle inequality gives the bound for the raw update. Non-expansiveness of clipping follows from the fact that projection onto a convex interval is 1-Lipschitz.*

Interpretation. Proposition 1 formalizes the numerical stability of the environment under exploratory control. The one-step map is Lipschitz, and the clipping operation is non-expansive, which together prevent uncontrolled amplification of small perturbations.

Appendix D.7. Summary

The proposed environment demonstrates the stability necessary for closed-loop benchmarking. The soil–water state remains physically bounded for all admissible actions and climatic forcing, ensuring positive invariance. Hydrological fluxes remain bounded under bounded drivers, reflecting bounded-input bounded-state (BIBS) stability. Additionally, the hybrid residual coupling preserves well-posedness under mild boundedness and invertibility assumptions.

Furthermore, the stability and well-posedness analysis establishes continuous dependence of the soil–water state on initial conditions, control inputs, and climatic forcing. This property is a necessary prerequisite for sensitivity analysis. Explicit analytical parametric sensitivity metrics are not derived in this appendix. Instead, sensitivity is investigated empirically through controlled scenario analyses, consistent with the control-oriented and benchmarking-focused scope of the model.

Collectively, these properties support the control-aware purpose of the formulation. The focus is on ensuring stable, interpretable, and reproducible closed-loop simulations under uncertainty, rather than replicating all fine-scale soil hydrodynamics.

References

Allen, R.G., Pereira, L.S., Raes, D., Smith, M., 1998. Crop Evapotranspiration: Guidelines for Computing Crop Water Requirements. FAO Irrigation and Drainage Paper 56, FAO, Rome.

Amarasinghe, K., Rodolfa, K., Lamba, H., Ghani, R., 2020. Explainable machine learning for public policy: Use cases, gaps, and research directions. Data & Policy 2, e20. doi:10.1017/dap.2020.19.

Bennett, N.D., Croke, B.F.W., Guariso, G., Guillaume, J.H.A., Hamilton, S.H., Jakeman, A.J., Marsili-Libelli, S., Newham, L.T.H., Norton, J.P., Perrin, C., Pierce, S.A., Robson, B., Seppelt, R., Voinov, A.A., Fath, B.D., Andreassian, V., 2013. Characterising performance of environmental models. Environmental Modelling & Software 40, 1–20. doi:10.1016/j.envsoft.2012.09.011.

Berkenkamp, F., Schoellig, A.P., Krause, A., 2017. Safe model-based reinforcement learning with stability guarantees. Advances in Neural Information Processing Systems 30, 908–918.

Beucler, T., et al., 2021. Implicit learning of convective organization explains precipitation stochasticity. Nature 597, 672–677. doi:10.1038/s41586-021-03860-w.

Bo, Y., Yan, Y., Chen, J., Liang, Y., Zhang, Y., Liu, Y., Zhang, Y., Zhang, Y., Zhang, Y., Zhang, Y., 2025. Process-based modeling framework for sustainable irrigation management at the regional scale: integrating rice

production, water use, and greenhouse gas emissions. Geoscientific Model Development 18, 3799–3818. doi:10.5194/gmd-18-3799-2025.

Fatichi, S., et al., 2016. Ecosystem and land surface modelling in a changing climate. Hydrology and Earth System Sciences 20, 455–478. doi:10.5194/hess-20-455-2016.

Fereres, E., Soriano, M.A., 2007. Deficit irrigation: A global perspective. Agricultural Water Management 80, 1–22. doi:10.1016/j.agwat.2005.07.014.

Giuliani, M., Castelletti, A., Pianosi, F., Mason, E., Reed, P.M., 2016. Coping with deep uncertainty in water management: Policy search under uncertainty. Environmental Modelling & Software 81, 60–74. doi:10.1016/j.envsoft.2016.02.006.

Giuliani, M., et al., 2021. Reinforcement learning and control of water systems: An overview. Environmental Modelling & Software 141, 105045. doi:10.1016/j.envsoft.2021.105045.

Hadka, D., Reed, P.M., 2013. Borg: An auto-adaptive many-objective evolutionary computing framework. Environmental Modelling & Software 37, 97–111. doi:10.1016/j.envsoft.2012.07.004.

Höge, M., Scheidegger, A., Baity-Jesi, M., Albert, C., Fenicia, F., 2022. Improving hydrologic models for predictions and process understanding using neural ODEs. Hydrology and Earth System Sciences 26, 5085–5106. doi:10.5194/hess-26-5085-2022.

Huang, Z., Wang, Y., Hui, C., XiaoCheng, 2025. An intelligent water-saving irrigation system based on multi-sensor fusion and visual servoing control. arXiv preprint arXiv:2510.23003. doi:10.48550/arXiv.2510.23003.

Jones, H.G., et al., 2022. Smart irrigation systems: A review of control strategies and technologies. Agricultural Water Management 260, 107300. doi:10.1016/j.agwat.2021.107300.

Karniadakis, G.E., et al., 2021. Physics-informed machine learning. Nature Reviews Physics 3, 422–440. doi:10.1038/s42254-021-00314-5.

Li, Z., Zhang, Y., Wang, J., Chen, X., Li, J., 2022. Deep learning for intelligent irrigation decision-making: A review. Agricultural Water Management 265, 107561. doi:10.1016/j.agwat.2022.107561.

Monteith, J.L., 1965. Evaporation and environment. Symposia of the Society for Experimental Biology 19, 205–234.

Padilla-Nates, J.P., Garcia, L.D., Lozoya, C., Orona, L., Cortes-Perez, A., 2025. Greenhouse irrigation control based on reinforcement learning. Agronomy 15, 2781. doi:10.3390/agronomy15122781.

Perkins, S., et al., 2023. Safe reinforcement learning for real-world control systems: A survey. IEEE Transactions on Artificial Intelligence 4, 1–18. doi:10.1109/TAI.2022.3220730.

Rackauckas, C., Ma, Y., Martensen, J., Warner, P., Zubov, K., Supekar, S., Skinner, D., Ramadhan, A., Edelman, A., Perdikaris, P., 2020. Universal differential equations for scientific machine learning. Proceedings of the National Academy of Sciences 117, 29041–29048. doi:10.1073/pnas.2001336117.

Rackauckas, C., et al., 2021. Scientific machine learning through physics-informed neural networks and universal differential equations. Computing in Science & Engineering 23, 18–31. doi:10.1109/MCSE.2020.3042241.

Raes, D., Steduto, P., Hsiao, T.C., Fereres, E., 2009. AquaCrop—The FAO Crop Model to Simulate Yield Response to Water. FAO, Rome.

Raffin, A., Hill, A., Gleave, A., Kanervisto, A., Ernestus, M., Dormann, N., 2021. Stable-baselines3: Reliable reinforcement learning implementations. Journal of Machine Learning Research 22, 1–8. URL: `https://www.jmlr.org/papers/v22/20-1364.html`.

Reichstein, M., Camps-Valls, G., Stevens, B., Jung, M., Denzler, J., Carvalhais, N., Prabhat, 2019. Deep learning and process understanding for data-driven earth system science. Nature 566, 195–204. doi:10.1038/s41586-019-0912-1.

Rodríguez-Iturbe, I., Porporato, A., 2004. Ecohydrology of Water-Controlled Ecosystems. Cambridge University Press.

Rolnick, D., et al., 2022. Tackling climate change with machine learning. ACM Computing Surveys 55, 1–96. doi:10.1145/3485128.

Seneviratne, S.I., et al., 2010. Investigating soil moisture–climate interactions in a changing climate. Earth-Science Reviews 99, 125–161.

Seneviratne, S.I., et al., 2021. Weather and climate extreme events in a changing climate. Nature Climate Change 11, 964–974. doi:10.1038/s41558-021-01092-9.

Staff, S.N., 2025. Climate change reduces crop yields worldwide even with adaptation. https://news.stanford.edu/stories/2025/06/climate-change-cuts-global-crop-yields Stanford Report.

Sutton, R.S., Barto, A.G., 2018. Reinforcement Learning: An Introduction. 2 ed., MIT Press, Cambridge, MA.

Verbruggen, W., Wårlind, D., Horion, S., Meunier, F., Verbeeck, H., Schurgers, G., 2025. Implementing a process-based representation of soil water movement in a second-generation dynamic vegetation model: application to dryland ecosystems (LPJ-GUESS-RE v1.0). EGUsphere , 1–28doi:10.5194/egusphere-2025-1259.

Vereecken, H., et al., 2007. Modeling soil processes: Review, key challenges, and new perspectives. Vadose Zone Journal 6, 749–762.

Willard, J., Jia, X., Xu, S., Steinbach, M., Kumar, V., 2022. Integrating physics-based modeling with machine learning: A survey. Nature Reviews Physics 4, 366–382. doi:10.1038/s42254-022-00437-4.

Yang, T., et al., 2021. Reinforcement learning for water resources management: A review. Water Resources Research 57, e2020WR028838. doi:10.1029/2020WR028838.